

**USMANU DANFODIYO UNIVERSITY, SOKOTO
(POSTGRADUATE SCHOOL)**

**CATALYTIC CONVERSION OF FURFURAL FROM HEMICELLULOSE OF
CITRULLUS COLOCYNTHIS L. (MELON) SEED HUSK TO LIQUID
HYDROCARBONS**

**A Dissertation
Submitted to the
Postgraduate School,
USMANU DANFODIYO UNIVERSITY, SOKOTO, NIGERIA**

**In Partial Fulfillment of the Requirements
for the Award of the Degree of
MASTER OF SCIENCE (PETROLEUM CHEMISTRY)**

By

**ABBA, Umar Aji
Adm. No.: 16210313004**

Department of Pure and Applied Chemistry

JANUARY, 2020

DEDICATION

This work is dedicated to the blessed memory of Late Alkali Mustapha Aji, Late Ahmad Muhammad Jaji, Late Hajiya Aisha Aji, Late Maryam Muhammad Jaji, Late Hajiya Aisha Musa Kyari, LateHajiya AishaAji (Mamma) and Late Alhaji Umar Bunu Abba.

CERTIFICATION

This dissertation by ABBA,UmarAji (Adm. No.: 16210313004) has met the requirements for the award of the degree of Master of Science (Petroleum Chemistry) of the UsmanuDanfodiyo University, Sokoto, and is approved for its contribution to knowledge.

(External Examiner)

Date

Dr. C. Muhammad
(Major Supervisor)

Date

Dr. M.N. Almustapha
(Co-Supervisor I)

Date

Dr. S.U. Dandare
(Co-Supervisor II)

Date

Prof. A.B. Muhammad
(Head of Department)

Date

ACKNOWLEDGEMENTS

This dissertation would not have been possible without the help of Almighty ALLAH (SWT), the most exalted who spared my life and gave me the opportunity to complete this work. May the peace and blessings of Allah be upon his servant and messenger, Muhammad son of Abdullah (S.A.W.).

It is a pleasure to express my gratitude to the great people behind the success of this work. First and foremost, to my Supervisory team Dr. C. Muhammad (Major Supervisor), Dr. M.N. Almustapha (Co- Supervisor I) and Dr. S.U. Dandare (Co- Supervisor II) for their invaluable guidance, encouragement, understanding, advise and professional approach towards the success of this work. It has been a privilege to work under their supervision and to experience their in-depth knowledge, endless passion for research, unique perspective and foresight.

Special appreciations go to Dr. A.M. Sokoto, Prof. A.B. Muhammad, Prof. U.A. Birnin-Yauri, Prof. L.G. Hassan Prof. B.U. Bagudo, Prof. U.Z. Faruq, Prof. A.I. Tsafe, Prof. S.M. Dangoggo, Dr. M.U. Dabai, Dr. M.G. Liman, Dr. M. M. Ladan, Dr. S.A. Zauru, Dr. Z.I. S.G. Adiya, Mal. A.S. Yelwa, Mal. J. Sani, Mal. S. Yahaya, Mal. A.I. Muhammad, Mal. I. Ibrahim, Mal. S.S. Adamu and entire staff members of Department of Pure and Applied Chemistry for their insightful comments and supports throughout my program.

I wish to express my profound gratitude and appreciation to my parents Alhaji Baba Abba Aji, Hajiya Fatima Muhammad Jaji and Hajiya Bilkisu Mustapha, without your unconditional support and prayers throughout my life and studies, i am sure i would not be where i am today. Thank you so much May ALLAH in His ultimate mercy rewards you with Jannatul firdaus and may He continue to bless your lives ameen.

Word cannot be enough to thank my beloved grandmother HajiyaAsiyaAji, my uncles and their families, Muhammad AuwalAji, Abubakar Aji, Hassan Aji, HussainiAji, IsiyakuAji, Alhaji KundaAji for their encouragement, advise and prayers through out my life may Allah reward you abundantly.

My deepest appreciation goes to my beloved brothers and sisters, Alhassan Abba Aji, Muhammad Ramadan, Muhammad AjiLamaraFatima Muhammad Abba, Aisha Muhammad Abba, Maryam Abba Aji, Asiya Abba Aji, Muhammad Aji Mustapha, Aisha Abba Aji, Muhammad Abba Aji, Mustapha Abba Aji, Zahra'u Abba Aji, Musa Abba Aji, Kaseem Abba Aji, Hassan Abba Aji, Hussaini Abba Aji, Fatima Abba Aji, Muhammad Abba Aji, Aisha Abba Aji, Fatima Abba aji (Ajuzz), and Fatima Muhammad Zarma fortheir love, support, encouragement and prayers, i wish you brilliant success in life.

Finally, yet importantly, I acknowledged the help, effort and enthusiasm ofGambo Muhammad, Mustapha Lawan Kar, Muhammad Yahaya, Sunusi Muhammad Sambo, Ibrahim HamisuMatazu, Shuaibu Hassan Jatau,Abdulgafar Usman and all members of 2016/2017 Postgraduate class of both Renewable Energy, Applied and Pure Chemistry for the amazing friendship we shared. May almighty Allah in his boundless mercy unite us all in the paradise in Heaven.

TABLE CONTENTS

TITLE PAGE.....	i
DEDICATION.....	ii
CERTIFICATION.....	iii
ACKNOWLEDGEMENTS.....	iv
TABLE OF CONTENTS.....	vi
LIST OF PLATES.....	viii
LIST OF FIGURES.....	ix
LIST OF SCHEMES.....	x
LIST OF TABLES.....	xi
ABBREVIATIONS.....	xii
ABSTRACT.....	xiii
CHAPTER ONE.....	1
INTRODUCTION AND LITERATURE REVIEW.....	1
1.1 Introduction.....	1
1.1.1 Biomass.....	2
1.1.2 Melon.....	2
1.1.3 Melon Seed Husk.....	3
1.1.4 Furfural.....	5
1.1.5 Synthesis of Furfural.....	5
1.2 Literature Review.....	9
1.2.1 Lignocellulosic Biomass.....	9
1.2.2 Production of Liquid Fuels from Biomass.....	10
1.2.3 Furfural Production.....	13
1.2.4 Aldol Condensation Reaction.....	15
1.2.5 Furfural Upgrade to Fuels and Conversion Processes.....	16
1.3 Research Problem.....	18
1.4 Justification.....	20
1.5 Aim and Objectives.....	21
1.6 Scope and Delimitation.....	21
CHAPTER TWO.....	22
MATERIALS AND METHODS.....	22
2.1 Materials.....	22
2.2 Sample Collection and Treatment.....	24
2.3 Methods.....	24

2.3.1 Reagents Preparation.....	24
2.3.2 Catalyst Preparation.....	25
2.3.3 Catalyst Characterisation.....	25
2.3.4 Experimental Design.....	26
2.3.5 Description of the Experimental Runs for Furfural Production.....	27
2.3.6 Data Analysis.....	28
2.3.7 Optimization and Validation of the Furfural Yield.....	29
2.3.8 Aldol Condensation of Furfural with Acetone.....	29
2.3.9 FT-IR Analysis of Furfural Produced and Furfural Acetone Adduct.....	30
2.3.10 Hydrodeoxygenation of Furfural Acetone Adduct to Hydrocarbon Fuels.....	30
2.3.11 GC-MS Analysis of Hydrodeoxygenated Product.....	31
CHAPTER THREE.....	33
RESULTS AND DISCUSSION.....	33
3.1 Effect of process Variables on the Furfural Yield.....	33
3.2 Response Optimization and Validation.....	41
3.3 Furfural Identification.....	42
3.4 Furfural Acetone Adduct Identification.....	43
3.5 NiO/SiO ₂ Catalyst Characterisation.....	44
3.6 GC-MS of Hydrodeoxygenated Product of Furfural Acetone Adduct.....	46
CHAPTER FOUR.....	48
CONCLUSION AND RECOMMENDATIONS.....	48
4.1 Conclusion.....	48
4.2 Recommendations.....	49
REFERENCES.....	50
APPENDICES.....	54

LIST OF PLATES

Plate 1.1: Melon Seed Husk.....	4
Plate 2.1: Set up for Furfural Production.....	28
Plate 2.2: Set up for Hydrodeoxygenation of Furfural-Acetone adduct to Hydrocarbon fuels	31

LIST OF FIGURES

Figure 3.1: Contour Plot Showing the Combined Effect of Acid Concentration and Reaction Time on Furfural Yield with the Reaction Temperature Held

Constant.....40

Figure 3.2: Contour Plot Showing the Combined Effect of Acid Concentration and Reaction Temperature on Furfural Yield with the Reaction Time Held

Constant.....40

Figure 3.3: Contour Plots Showing the Combined Effect of Reaction Time and Reaction Temperature on Furfural Yield with the Acid Concentration Held

Constant.....41

LIST OF SCHEMES

Scheme 1.1: Synthesis of Furfural.....	6
Scheme 1.2: Chemical Transformation of Biomass to Liquid Hydrocarbons.....	11
Scheme 1.3: Transformation of Furfural into Fuel Additives and Liquid Alkanes.....	17
Scheme 2.1: Condensation of Furfural with Acetone.....	30

LIST OF TABLES

Table 2.1: List of Chemicals and Solvents.....	22
Table 2.2: List of Apparatus/Instruments.....	23
Table 2.3: Process Variables and their Levels used in the Central Composite Design.....	26
Table 3.1: Central Composite Design for the Furfural Production.....	34
Table 3.2: Results of Analysis of Variance (ANOVA) for Furfural Yields(%).....	36
Table 3.3: Results of Regression Analysis showing Estimated Coefficients of the Model and theirSignificance.....	38
Table 3.4: Predicted Results of Optimization and Validation of Melon Seed Husk Furfural Yields.....	42
Table 3.5: XRF Results of NiO/SiO ₂	45
Table 3.6: Composition of HydrodeoxygenatedProduct.....	47

ABBREVIATIONS

2-MTHF	2-Methyltetrahydrofuran
2-MF	2-Methyl Furan
BCT	Biomass Conversion Technology
DMF	2,5-dimethylfuran
FAA	Furfural Acetone Adduct
FT-IR	Fourier transform infrared
GHGs	Green House Gases
HAA	HydroxyAlkylation/Alkylation
HDO	Hydrodeoxygenation
HMF	Hydroxymethylfuran
MSH	Melon Seed Husk

MSO	Melon Seed Oil
LCT	Low Carbon Technology
XRF	X-ray Fluorescence

ABSTRACT

Catalytic Conversion of Furfural from Hemicelluloses of *CitrillusColocynthis L.* (Melon) Seed Husk to Liquid Hydrocarbons over NiO/SiO₂ was investigated. A central composite design was used for furfural production, using response surface methodology, a furfural with optimum yield of 75.03% was achieved by acid-catalyzed hydrolysis/dehydration of Melon Seed Husk at Temperature (220 °C), Acid Concentration (10% H₂SO₄), and Reaction Time (55 minutes) which was subsequently converted to liquid hydrocarbons via Furfural-Acetone condensation followed by Hydrodeoxygenation of Furfural-Acetone Adduct. FT-IR spectrum of the produced furfural showed absorption at 1670 cm⁻¹ and 2800 cm⁻¹ indicating a conjugated carbonyl functional group and aldehydic hydrogen. The Hydrodeoxygenation was carried out in a stainless-steel reactor at 150 °C for 8 hours. The NiO/SiO₂ catalyst for Hydrodeoxygenation reaction was prepared by wet impregnation method. XRF analysis of the NiO/SiO₂ revealed a Percentage Metal oxide Composition of 73.939% SiO₂ and 24.641% NiO. The Hydrodeoxygenation using NiO/SiO₂ in water at 150 °C for 8 hours yielded liquid hydrocarbons with 86.61% hydrocarbons yield (C₉-C₁₂) and 1.46% 2-propenylidenecyclobutene. The result revealed that *Citrullus Colocynthis L.* (Melon) Seed Husk is a good source for furfural and liquid hydrocarbons production and could be used as a feedstock in industries for fuel and chemical production.

CHAPTER ONE

INTRODUCTION AND LITERATURE REVIEW

1.1 Introduction

Humanity is now faced with the challenges of the increasing demand for fuels and chemicals driven by global population growth and diminishing fossil resources, energy security due to political issues, and environmental problems caused by CO₂ emissions and the resulting global warming. To solve these, various forms of renewable energy resources have been explored to develop sustainable processes. Different from other energy sources such as, solar, wind and geothermal; biomass is the most promising alternative resources since it can provide the liquid fuels directly by a sequence of chemical reactions (Clark *et al.*, 2006).

Biomass, a renewable non fossil carbon energy source, is regarded as an ideal alternative to traditional fossil resources because it is environmentally friendly and abundant. In recent decades, great interest has been devoted to the production of biofuels and biochemicals using non-edible lignocellulosic biomass, which is abundant in agricultural residues and waste streams. (Perlack *et al.*, 2005).

The use of lignocellulosic biomass avoids the food-versus-fuel debate and can potentially significantly reduce CO₂ emissions. It is one of the most promising options for the green and sustainable production of fuels and chemicals. Lignocellulosic biomass mainly contains cellulose, hemicellulose, and lignin, which constitute 40–50%, 25–35%, and 15–20% of lignocellulose respectively. (Clark *et al.*, 2006)..

Transportation fuels such as gasoline, diesel, and jet fuel are the main targets of biofuels. Bioethanol as bio-gasoline and fatty acid alkyl esters as biodiesel are now commercialized on a large scale. However, these “first-generation” biofuels have problems such as low energy density, low stability, and sometime conflict with food production. To overcome these problems, intense work has been undertaken to develop next-generation biofuels that are produced from nonfood biomass such as Melon Seed Husk and are totally compatible with petroleum-based transportation fuels composed of hydrocarbons.

1.1.1 Biomass

Biomass is a renewable energy generated from animal and plant organic matter. Though, when utilized tends to generate carbon dioxide. It was also created from solar energy, water, carbon dioxide and does not increase net carbon dioxide volume in the earth, as such biomass can be regarded as carbon neutral (Kamimoto, 2008).

1.1.2 Melon

Melon (*Citrullus Colocynthis L.*) is a tropical herbaceous, tendril-bearing, vine plant of the *cucurbitaceae* family commercially cultivated in various regions in Africa (more especially Northern Part of Nigeria). It is an essential perennial cash crop cultivated for its fruits and oil-bearing seeds, the fruits are ovoid shaped and weighs an average of 1.5kg. The mesocarp comprises numerous brown coloured oval shaped, *dorsoventrally* flattened seeds enclosed in a brittle cortex. The seeds contain a white, soft textured oil-rich kernel that is typically dehulled for processing into melon seed oil (MSO). The oil content of melon seed ranges from 22.10 to

53.50% along with a crude protein content of 21.8%. The oil is an important feedstock used for various food, Medicinal, biodiesel fuel, pesticides, and industrial purpose (Nyakuma, 2015b).

1.1.3 Melon Seed Husk (MSH)

Melon Seed Husk (MSH) is the oval shaped, brown colored, outer coat, generated from decortication of the melon seeds. With the growing culinary and medicinal importance of melon seeds, it is estimated that the cultivation and extraction of Melon Seed Oil (MSO) will result in increased wastes over the coming years (WorldWatch Institute, 2017). This will present further waste disposal and management challenges for the communities reliant on the crop for livelihood. In addition, current strategies (open air burning, incineration, and deposition in land fill sites and refuse dumps) for the disposal and management of agricultural wastes such as Melon Seed Husk are considered inefficient, unsustainable, and environmentally hazardous (Nyakuma, 2015). Therefore, practical solutions are urgently required to significantly address problems associated with fossil fuels, the potential challenges of greenhouse gas (GHGs) emissions, global warming, and climate change resulting from fossil fuels combustion, open air burning, land filling, and dumping of agro forestry wastes into the environment.



Plate 1.1: Melon Seed Husk

Source: Author's field work 2019

The utilization of Melon Seed Husk (MSH) as fuel feedstock for biomass and bioenergy applications is a potential solution for the current waste management strategies for disposing MSH and addresses fossil fuels environmental challenges. The value addition of MSH can be achieved through biomass conversion technologies (BCT). This can be achieved by employing practical to energy technologies such as torrefaction, pyrolysis and gasification (Nyakuma, 2015). The application of the outlined low carbon technologies (LCT) can potentially address the challenges associated with fossil fuels by producing clean and renewable transportation fuel, mitigate the uncontrolled emission of GHGs from combustion of fossil fuels and burning of waste disposable biomass of melon seed oil extraction, land filling and reduce the associated costs of managing solid wastes such as MSH in the future (Nyakuma, 2015). Upgrading of lignocellulosic biomass into transportation fuel fractions have been intensively studied by catalytic hydrogenation-deoxygenation of furfural-Acetone condensation adduct as chemical precursor (Huber *et al.*, 2006).

1.1.4Furfural

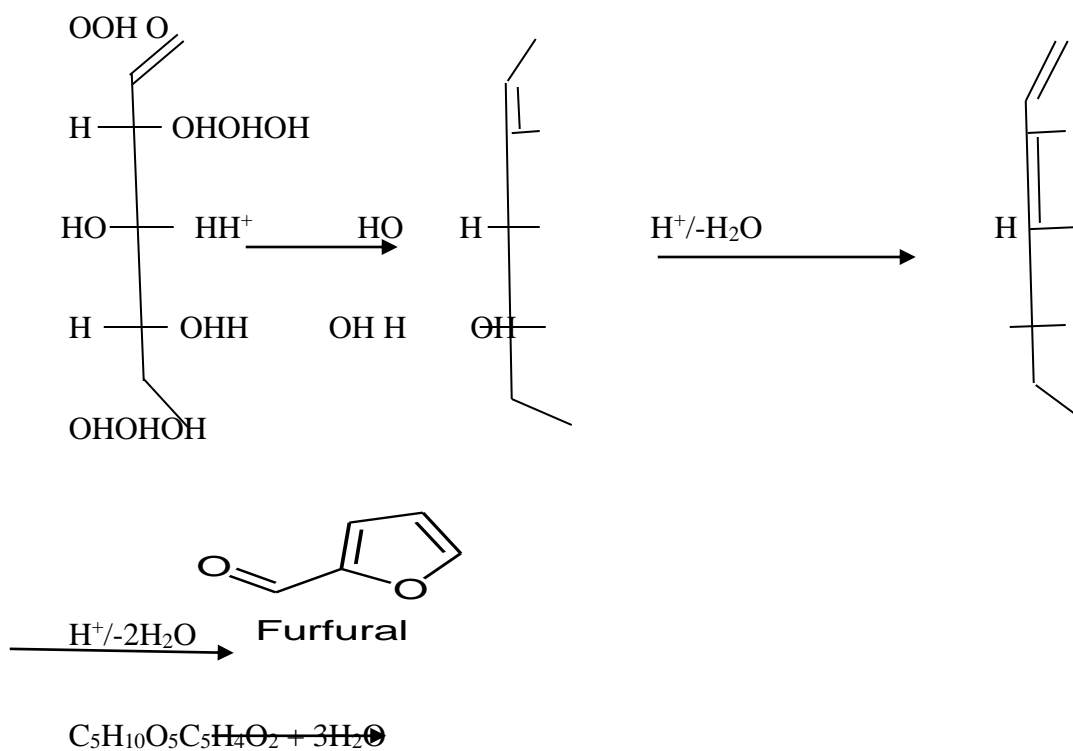
Furfural is a liquid chemical that is sourced from renewable resources; it is created from hemicelluloses components (pentosans) of vegetable matter. It is also the only compound of the furan series being directly obtained from biomass(e.g. Melon Seed Husk) at industrial scale. Furfural production is generally carried out by hydrolysis of hemicelluloses-derived pentosans into monomeric pentoses, and their subsequent acid-catalyzed dehydration. It is an important organic chemical, produced from agro industrial wastes and residues containing carbohydrates known as pentosans (Gebreet *et al.*, 2015)

As no commercial synthetic routes have been found so far, all furfural manufacturing activity is based on pentosans containing residues that are obtained from the processing of various agricultural and forest products. In commercial terms the most important intermediate derived from furfural is furfuryl alcohol. The chemical formula for furfural is $C_5H_4O_2$. In structure, it is a heterocyclic compound consisting of a furan ring (four carbon atoms and an oxygen atom) plus an aldehyde group. Chemically, furfural participates in the same kinds of reactions as aldehyde and other aromatic compounds. Indicating its diminished aromaticity relative to benzene, furfural is readily hydrogenated to the corresponding tetrahydrofuran derivatives.

1.1.5Synthesis of Furfural

Furfural can be produced from lignocellulosic biomass by dehydrating pentoses which are found in hemicelluloses of agricultural waste. The pentosans fraction of

lignocelluloses is converted into monosaccharide by acid hydrolysis. Then further dehydration reactions of pentoses yield furfural. Pentosan ($C_5H_8O_4$) fraction of melon seed husk is converted into pentose ($C_5H_{10}O_5$) which is then cyclodehydrated to furfural ($C_5H_4O_2$) using dehydration method. Dilute sulphuric acid is used for this purpose. Furfural formed is recovered using distillation and separation.(Ong and Sashikala, 2007). The stoichiometric equation for this reaction is as below:



(Pentoses)(Furfural)

Scheme 1.1: Formation of Furfural from Pentose (Ong and Sashikala, 2007).

The monomer/dimer furanyl derivatives (C_8 - C_{15}) are formed when condensation of furfural was carried out with ketone/aldehydes. Valuable liquid hydrocarbons are

obtained from this reaction (Condensation reaction) by converting the complex molecules with ketonic C=O, aliphatic C=C, Furanic C=C bond (Ulfa *et al.*, 2017).

Hydrodeoxygenation (HDO) is an effective method for the removal of oxygen from hemicellulose derived aldol adduct (Zhang *et al.*, 2013). Bifunctional catalyst comprised of active metal and solid acid exhibits excellent activity for HDO reaction. Normally, it is considered that the metal acts as hydrogenation activity center while the support provides acid sites for HDO reaction (Zhang *et al.*, 2013).

The selection of catalyst plays an important role. Among different metal loading, the noble metal such as platinum (Pt) and palladium (Pd) have been revealed as suitable metals for hydrogenation reaction (Fabaet *et al.*, 2012). Furthermore, since HDO of bio-fuel is expected to be a large-scale process, employment of noble metal-based catalysts could significantly raise production costs. However, the high prices of these noble metals failed to impress the industrial scope. As a consequence, the development of non-noble metal catalyst seems more rational. Thus, it seems more reasonable to use Ni-based catalyst for bio-fuel production via HDO owing to its lower cost (Ulfa *et al.*, 2017).

Apart from the active metal, support material is also the key factor determining the catalytic performance. In the past, Al₂O₃ was widely used as catalyst support for HDO due to its cheap cost, excellent texture, and suitable acidity. However, coke formation tends to occur because of the induction of acid sites during HDO (Ulfa *et al.*, 2017). Catalyst activity usually disappeared swiftly because large amount of coke formed during the HDO reaction process. Worse, part of Al₂O₃ can be

transformed into bohmite under hydrothermal conditions because alumina is known to be metastable under hydrothermal conditions, which usually lead to a decrease for catalytic activity. To overcome these drawbacks, one of the major challenges in HDO reaction is to find suitable catalyst support. Recently numerous support materials such as active carbon, ZrO_2 and TiO_2 were explored (Ulfaet *al.*, 2015).

Onwudili *et al.*, (2018) reported the influence of Si/Al ratio on the pyrolysis-catalysis of a simulated plastic sample for the production of upgraded fuels and chemicals. The yield of the product oil decreased with the addition of the catalysts, but the oil was of significantly lower molecular weight range, containing a product slate of premium fuel range $\text{C}_5\text{-C}_{15}$ hydrocarbons.

SiO_2 is an inert material with excellent hydrothermal stability, and had been used as a catalyst support in the HDO of organic compounds. For example, Pt catalyst supported on SiO_2 was used in the HDO of cresol and guaiacol, obtaining high hydrocarbon yields (Zhan *et al.*, 2017).

To overcome these problems mentioned above, thus, in this research work, an inexpensive non-sulfided HDO catalyst was prepared by impregnation using the pristine transition metal Ni (nickel) as the active component and SiO_2 (silica) as support. The aim is to convert diverse hemicellulose derived furfural of melon seed husk into liquid hydrocarbons via Hydrodeoxygenation (HDO). The catalytic conversion of melon seed husk to liquid hydrocarbons via hydrogenation followed by deoxygenation is proposed in one-step reaction using NiO/SiO_2 catalyst. The use of SiO_2 was reported increasing the activity of the catalyst by decreasing carbon

deposition on the surface of catalyst which lead to the formation of oxygenated compounds (Zhanget *al.*, 2014). The crystal structure of SiO₂ is relatively stable in water and organic solvent. Hence, the reaction under liquid phase is favorable.

1.2 Literature Review

1.2.1 Lignocellulosic Biomass

In general, lignocelluloses biomass can be defined as a renewable resource that can be transformed and used for the production of fuels or transformed into bioenergetic form for final use. Because of its abundance, availability and renewable character it serves as a promising feedstock for bio-fuels, bioenergy, biomaterials, and biochemical production(Machadoet *al.*, 2016).

Energetic crops, industrial residues, forestry and urban residues and agricultural residues are the major sources of biomass. Example of energetic crops are hybrid willow, sunflower and barley, they are generally densely cultivated, have high production and short rotation while agricultural residue comprised of stalk and leaves which are not collected in commercial crops such as rice straw, bagasse saccharine sorghum. Moreover, biomass that not collected from logging site as well as from forest management operations are refers to as forestry residues while solid residues, sewage sludge and industrial residues are termed as industrial and urban residues (Machadoet *al.*, 2016).

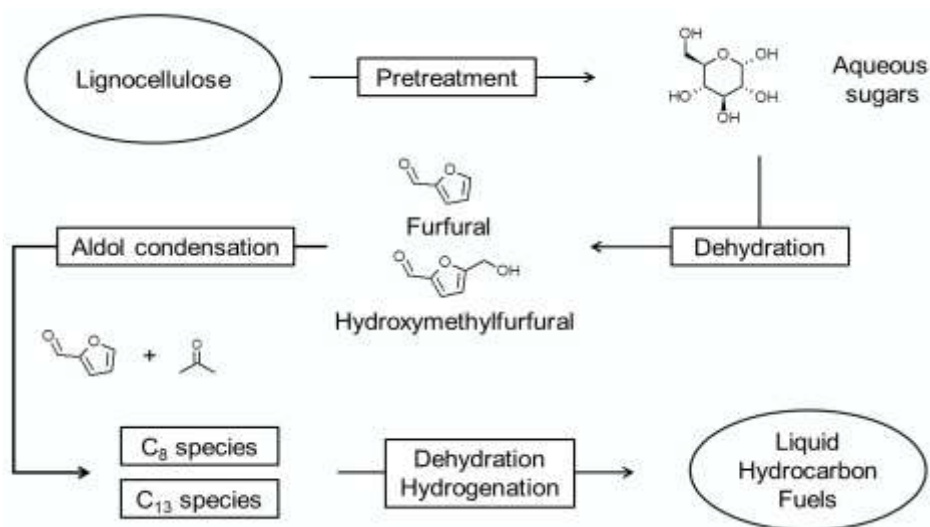
Solar is used by plant to form a sugar building block (which is stored in a polymer form as cellulose, starch, or hemicellulose) and oxygen by combining carbon

dioxide and oxygen. Most biomass approximately contained 75 wt % sugar polymers (Huber *et al.*, 2006).

The first step for biofuels production is obtaining an inexpensive and abundant biomass feedstock. Biofuel feedstocks can be chosen from the following: waste materials (agricultural wastes, crop residues, wood wastes, urban wastes), forest products (wood, logging residues, trees, shrubs), energy crops (starch crops such as corn, wheat, barley; sugar crops; grasses; woody crops; vegetable oils; hydrocarbon plants), or aquatic biomass (algae, water weed, water hyacinth). The structured portion of biomass is composed of cellulose (35-50%), hemicelluloses (20-35%), lignin (15-25%) and a number of other compounds (Cormaet *et al.*, 2007).

1.2.2 Production of Liquid Fuels from Biomass

The catalytic sequence for the production of liquid fuels from biomass is proposed to be by dehydration of biomass, condensation reaction and hydrogenation and/or deoxygenation reaction. The dehydration of biomass gives furfural, the five-membered ring heterocyclic compounds with one carbon replaced by oxygen. The direct conversion of furfural fails to give long chain hydrocarbon derivatives except for the formation of gaseous (Sitthisaet *et al.*, 2011) In order to get the longer carbon chain, the condensation of furfural with ketone/aldehyde is subjected to give monomer/dimer of furanyl derivatives with carbon chain varied from C₈ to C₁₅. The condensation products contain conjugated ketone C=O, aliphatic C=C, and cyclic C=C furan bond which can be converted into liquid hydrocarbons through catalytic hydrodeoxygenation reaction (HDO) reaction (Faba *et al.*, 2014); (Mahfud *et al.*, 2016) ;(Ulfaet *et al.*, 2018).



Scheme 1.2: Chemical Transformation of Biomass to Liquid Hydrocarbons (Rong *et al.*, 2010)

Based on the background, a synthetic strategy to produce diesel-like hydrocarbon via catalytic HDO reaction has been intensively examined. The catalyst screening showed that noble metal catalysts, such as Pd and Pt are the most promising selective metal catalyst for HDO reaction (Fabaet *al.*, 2016). However, the industrial scope for the utilization of noble metal-based catalyst such as Pd and Pt tends to be too expensive and uneconomical. Compounds with low boiling point tends to be absorbed on the active of Pd catalyst which promote the deactivation of the catalyst. Meanwhile, nickel as a non-noble metal catalyst has the promising properties for Hydrodeoxygenation by the selectivity over C=C bond and low-cost production (Mahfud *et al.*, 2016).

The use of support is also important to increase the activity of the catalyst. Oxides support catalyst seems to be a more promising alternative due to their wide surface area, a combination of their acidic and basic sites properties, and have moderate

hydrothermal stability. The oxides with different types of acidic sites and strengths are interesting matrices from a catalytic point of view (Zhang *et al.*, 2014)

Garbaet *al.*, (2019) reported a number of viable options which are being explored for the production of energy to meet growing global energy demand. The research investigated the conversion of millet husk to liquid hydrocarbons. Furfural was produced from millet husk via a single-stage process that involved simultaneous hydrolysis and dehydration processes, and was subsequently converted to straight-chain hydrocarbons through Aldol condensation and Hydrodeoxygenation reactions. The Hydrodeoxygenation of the Aldol condensation product over NiO/Al₂O₃ (493 K, 30 bar and reaction time of 1 hour) yielded liquid hydrocarbons with the selectivity of 77.5%.

Wang *et al.*, (2015) investigated a new route for biomass derived aviation fuel synthesis by catalytic conversion in aqueous phase. Furfural with the yield of 71% was produced by acid hydrolysis of raw corncob, and hydrogenated to 2-methylfuran obtaining a yield of 89% over Raney Ni catalyst, both of which were implemented under mild reaction conditions. The Hydroxyalkylation/alkylation condensation of 2-methylfuran and furfural to C₁₅ intermediate was conducted by using organic and inorganic acid as the catalyst under the reaction condition of 328 K and atmospheric pressure. The maximal 95% of the C₁₅ intermediate was gained when using sulfuric acid as the catalyst. 83% of liquid alkanes (C₈-C₁₅) yield and more than 90% of C₁₄/C₁₅ selectivity were produced by hydrodeoxygenation of the C₁₅ intermediate.

Muhammad *et al.*, (2015) investigated a fuel production using two way-stage fixed bed reactor and determined the product yield, composition and hydrocarbon distribution obtained from real-world waste plastics, simulated mixed plastics and four virgin plastics in the presence of a zeolite HZSM-5 catalyst. For the uncatalysed pyrolysis of the plastics, a high yield of oil/wax was obtained for the plastic materials in the range of 81-97wt% . The yield of the oil/wax decreased with addition of catalyst to between 44 and 51 wt % . However, the composition of the oils was significantly increased in aromatic hydrocarbon content. In addition, the composition of the oils was shifted from molecular weight hydrocarbon (C_{16+}) to fuel range hydrocarbons (C_5-C_{15}) with a high content of single ring aromatic hydrocarbons such as benzene, toluene, ethylbenzene, xylenes and styrene.

1.2.3 Furfural Production

Xylans, one of the types of hemicelluloses present in abundance in lignocellulosic biomass, are composed mainly of pentose which are generally the major constituents of hemicelluloses in grasses and woods. Lately, studies focusing on the conversion of xylans to bioenergy, chemicals and biomaterials have received a lot of attention in the context of bio refineries. Among the products which can be obtained from pentose, there are furfural, which is a promising alternative, since it is a versatile compound that can be used in the synthesis of several other important chemicals, such as furan and furfural alcohol, furfural acetate, tetrahydrofuran, 2-methylfuran, and 2-methyltetrahydrofuran and it is vastly used in several applications in refining oil, plastics production, pharmaceutical and agrochemical industries (Wang *et al.*, 2015)

Furfural is commercially produced in batch or continuous processes using mineral acids as catalysts, even though this process presents drawbacks in the form of corrosion, difficulty in recovering the catalyst and the product from reaction mixture and risks to health and the environment. Aiming to optimize furfural production processes, several studies have been done involving the use of new types of catalysts in monophasic and biphasic reaction systems. Considering some organic solvents tested in biphasic systems that can increase the yield and selectivity of furfural, 2-methyltetrahydrofuran has been shown to be a good option.

This compound can be prepared from lignocellulosic biomass and easily separated from the aqueous phase due to its low solubility in water, stability in acid and alkaline conditions, low toxicity, easy recyclability and environmentally friendliness characteristics, because it is a product from green chemistry. Besides improving reaction system, it has been studied the use as catalysts which do no harm so much the environment as the mineral acids. (Li *et al.*, 2015)

In order to replace the use of mineral acids in furfural production, in recent years, many heterogenous catalyst were developed and applied successfully in the reaction for furfural preparation. One of the problems about using heterogenous catalyst is when the reaction solvent is too polar and highly protic, as water for example, because only a few heterogenous catalyst can keep the desired acidity due to interactions between solvent-surface by solvation.

Sokoto *et al.*, (2018) investigated the furfural production from millet husk via simultaneous hydrolysis and dehydration processes. Effect of reaction variables

such as temperature (120–200°C), resident time (15–45 min), and acid concentration (5–10%) was studied using central composite design. Furfural yield of 71.55% was achieved at 184 °C, 39 min, and 9% acid concentration. FT-IR spectrum of the produced furfural showed absorption at 1,697 and 2,880 cm⁻¹ indicating a conjugated carbonyl functional group and aldehydic hydrogen.

Chen (2015) developed a new method of furfural production using the liquor obtained after steam explosion pretreatment of rice straw, using as acid solid catalyst HZSM-5 Zeolite. In order to improve process efficiency, it was added to the reaction mixture a polymerization inhibitor, 4-methoxyphenol, which improved conversion of rice straw liquor in furfural.

Another study involving Zeolites use as acid catalyst was developed by Gao (2014) in which aqueous waste hemicelluloses solutions were used along with ZSM-5 Zeolite, being proved the catalyst stability and the possibility of its reuse.

1.2.4 Aldol Condensation Reaction

Aldol condensations and hydroxyalkylation-alkylation (HAA) reactions are two effective methods to extend the carbon chain length for furfural upgrading to fuels. Similar to Hydroxymethylfuran (HMF), furfural can also undergo aldol condensation with external carbonyl-containing molecules having an α -hydrogen (e.g. Ketones) in the presence of a base or an acid catalyst. Further hydrogenation of aldol products can produce high-quality longer-chain alkanes. The Dumesic group developed a sequential aldol-condensation and hydrogenation strategy for furfural upgrading in the aqueous phase using a bifunctional Pd/MgO–ZrO₂ catalyst

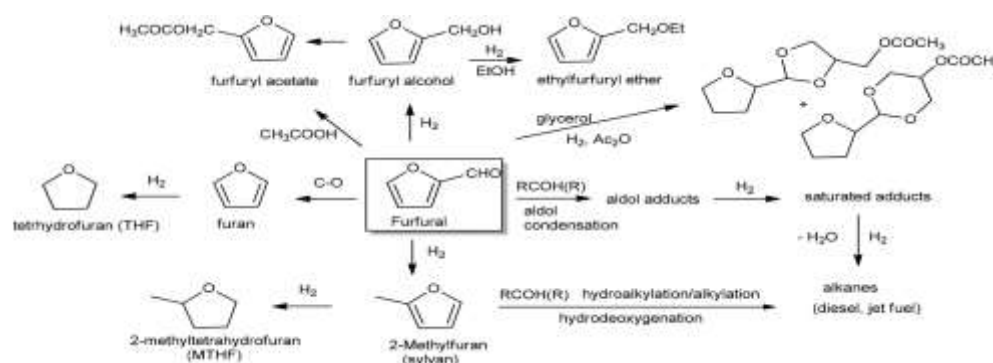
(Barrett *et al.*, 2016). The cross aldol-condensation of furfural with acetone results in water-insoluble monomer and dimer products, which are subsequently hydrogenated to give products with high overall carbon yields (>80%).

Seoet *al.*, (2018) reported Two-step hydrodeoxygenation of furan trimmers using supported Ni catalysts by substituting with noble metal catalyst (Pd/C) and (Ru/tungstate Zirconia). The substitution of the noble metal catalyst was successful leading to good HDO activity. A maximum theoretical yield of 87.9% of the oil phase product was achieved by the combination of the first step of Ni/CeO₂ (Hydrogenation) and the second step of Ni/tungstate zirconia (hydrodeoxygenation). Although more cracking of hydrocarbon product observed over the Ni catalyst (Seoet *al.*, 2018).

1.2.5 Furfural Upgrade to Fuels and Conversion Processes

Furfural is considered as a platform chemical for the production of liquid hydrocarbons and gasoline additives such as 2-methyltetrahydrofuran (2-MTHF).

Hydrogenation remains the most versatile reaction to upgrade furanic components to biofuels. For instance, it can lead to promising gasoline blends including 2-methylfuran (2-MF), 2,5-dimethylfuran (DMF) and 2-methyltetrahydrofuran (2-MTHF). Synthesis of biofuel components, including DMF from biomass and biomass derived carbohydrates via Hydroxymethylfuran (HMF) platform chemical has received significant attention in the recent years. (Yantao, *et al.*, 2019.)



Scheme 1.3: Transformation of Furfural into Fuel Additives and Liquid Alkanes (Corma *et al.*, 2014).

Sitthisa *et al.*, (2011), investigated conversion of furfural using Ni-Fe bimetallic and SiO_2 -supported Ni under process condition of 1 bar H_2 in the 210-250 °C temperature range. Hydrogenation and decarbonylation of the furfural results in the formation of furfuryl alcohol and furan as primary products over monometallic Ni/ SiO_2 , while Fe-Ni bimetallic catalyst increased 2-methylfuran (2-MF) yields with reduced in the furan yields and C_4 products. The results shows that C=O hydrogenation and C-O hydrogenolysis were promoted at low temperature and higher temperature respectively by the addition of Fe which suppressed the decarbonylation activity of Ni.

In another report, vapor phase furfural hydrogenation studies were performed on a series of silica supported mono disperse Pt nanoparticle catalysts where the extent of decarbonylation and hydrogenation of carbonyl group was highly dependent on the size and shape of Pt nanoparticles (NPs). Small particles were found to predominantly give furan as major product (via decarbonylation) while larger sized particles yielded both furan and furfuryl alcohol (carbonyl hydrogenation product).

Octahedral particles were found to be highly selective towards furfuryl alcohol, while cube-shaped particles produced an equal amount of furan and furfuryl alcohol. Furan and furfuryl alcohol were further converted to propylene and 2-methylfuran via decarbonylation and hydrogenolysis, respectively (Pushkarevet *al.*, 2012).

The authors suggested that the aromatic ring hydrogenation reactions for both furfural and furan-based compounds do not readily occur on Pt under the investigated conditions, most probably due to the poisoning of Pt surface with chemisorbed CO produced during furfural decarbonylation.

A comparative study for furfural hydrodeoxygenation using three different metal catalysts, Cu, Pd and Ni supported on SiO₂, revealed that products distribution was strongly dependent on the metal catalyst. A high selectivity to furfuryl alcohol was obtained for Cu/SiO₂ (with a small amount of 2-MF) as compared to furan decarbonylation observed followed by further hydrogenation to form THF in the case of Pd/SiO₂. Comparatively, Ni/SiO₂ promoted ring opening reactions to form butanal, butanol and butane in significant quantities.

1.3 Research Problem

As concern grows over the twin challenges of climate change and energy security (Diminishing Fossil Fuels resources), a number of viable options are being explored for the production of energy to meet the Global demand in sustainable fashion (Garbaet *al.*, 2019). The cultivation and extraction of vegetable oil from melon seeds generates large quantities of lignocellulosic waste known as Melon Seed

Husk (MSH). With the growing culinary and medicinal importance of melon seeds, it is estimated that the cultivation and extraction of Melon Seed Oil will result in increased waste over the coming years(world watch institute, 2017). This will present further waste disposal and management challenges for the communities reliant on the crop for livelihood. In view of this, there is an urgent need to explore new sustainable alternatives for valorizing and utilizing Melon seed husk (MSH).

The exploitation of biomass for energy and biochemical production has been recognized as a viable option for adding value to lignocellulosic agricultural residue such as corn stover, wheat straw, rice husk/straw, and millet husk with varying degree of success (Garba *et al.*, 2019). Therefore, it is suggested that an alternative, albeit potentially more efficient waste disposal strategy and management of MSH is the utilization of Melon Seed Husk as a feedstock for clean energy fuels and power generation. Hence, this could be achieve by converting the furfural from hemicelluloses of *Citrullus Colocynthis L.* (Melon) Seed Husk (MSH) to liquid hydrocarbons which are found in the hemicellulose of agricultural waste. However, this will serve as an alternative of transportation fuels from fossil fuels, potentially mitigate the uncontrolled emission of greenhouse gases (GHGs) from fossil fuels combustion and Open air burning, landfilling and reduce the associated costs of managing solid wastes (Baktash *et al.*,2015).

Several work were reported in the literature on the production of liquid hydrocarbons and effect of reaction conditions from lignocellulosic biomass, such as Concorbs (Wang *et al.*, 2015) and Millet husk (Garba *et al.*, 2019). To the best of our knowledge there is no published information in literature on the production of

liquid hydrocarbons from Furfural of Hemicelluloses of *Citrullus Colocynthis* L.(Melon) Seed Husk, therefore this research intend to produce liquid hydrocarbons from Furfural obtained from Hemicelluloses of *Citrullus Colocynthis* L.(Melon) Seed Husk via Hydrodeoxygenation using NiO/SiO₂ as a catalyst.

1.4 Justification

Melon seed husk which is a non-edible material, contains higher heating value than value reported for other lignocellulosic biomass fuel in the literature. this is primarily due to the high Carbon, Volatile matter, fixed carbon which accounts for the combustible content of MSH. The low N and S contents indicates that the thermal conversion of MSH will potentially result in low emissions of nitrous, sulfur oxides and other greenhouse gases (GHGs) into the atmosphere during thermal conversion (Nyakuma, 2015). This effectively highlights the environmentally friendly potential of the Melon seed husk (MSH) as a potential biomass fuel for future thermochemical application. However, conversion of Melon Seed Husk to liquid hydrocarbons presents opportunities for the production of clean, renewable and sustainable energy, fuel and chemicals. Likewise, potentially viable strategy for the efficient disposal and management of future agricultural waste stream and may also help create job for the teaming jobless youth.

1.5 Aim and Objectives

The aim of this research work is to produce liquid hydrocarbons from *Citrullus Colocynthis* L.(Melon) Seed Husk via Catalytic Hydrodeoxygenation of Furfural derivatives using NiO/SiO₂ catalyst.

The objectives of the research are to;

- I. Produce Furfural from Melon Seed Husk.
- II. Optimize Furfural Production from Hemicellulose of *Citrullus Colocynthis* L.(Melon) Seed Husk.
- III. Prepare and Characterize Catalyst for Hydrodeoxygenation Process
- IV. Convert the Produced Furfural into Hydrocarbons
- V. Determine the Chemical Composition of the generated Liquid Hydrocarbons

1.6 Scope and Delimitation

The scope of this research focuses on the production of liquid hydrocarbons from hemicellulose of Melon seed husk using NiO/SiO₂ catalyst via Hydrodeoxygenation Reaction. However, emphasis was made to optimize the furfural production process and determine the chemical compositions of the liquid products. However, the research will not account for the studies of the thermo gravimetric and kinetics of the melon seed husk, optimization of other reaction stages and the gases that were produced during the process.

CHAPTER TWO

MATERIALS AND METHODS

2.1 Materials

The chemical reagents/solvents and apparatus/Instruments used are listed in **Table 2.1** and **Table 2.2** below:

Table 2.1: List of Chemicals and Solvents

Chemicals/solvents	Chemical formula	Purity	Grade	Manufacturer
Sulphuric acid	H ₂ SO ₄	97.0	A.R	British Drug House
Sodium chloride	NaCl	99.5	A.R	LOBA Chemie Pvt India
Dichloromethane	CH ₂ Cl ₂	99.0	A.R	E-Merck Darmstadt
Sodium sulphate	Na ₂ SO ₄	99.0	A.R	LABTECH Chemicals
Sodium hydroxide	NaOH	97.0	A.R	LOBA Chemie Pvt India
Ethanol	C ₂ H ₅ OH	95.0	G.P.A	Kermel
Acetone	(CH ₃) ₂ CO	99.0	A.R	LOBA Chemie Pvt India
Ethyl acetate	CH ₃ COOC ₂ H ₅	99.5	A.R	LOBA Chemie Pvt India
Hydrated nickel nitrate	Ni(NO ₃).6H ₂ O	99.9	A.G	E-MERCK DARMSTADT
Silica	SiO ₂	99.5	A.R	LOBA Chemie Pvt India

Key: A.R=Analytical reagent, A.G=Analar Grade

Table 2.2: List of Apparatus/Instruments

Instruments/Apparatus	Model	Manufacturer
Analytical Balance	AW320	Shimadzu Japan
Hot plate with Magnetic Stirrer	ERC-1000H	Tokyo Rikakikai Co. Ltd, Japan
Glass Tubular Reactor	SS316L	Fabricated in India
Rotary Evaporator	SB-1100	Shanghaieyela (Tokyorikakika Co. Ltd China)
Laboratory oven	SM9053	Surgifriend Med., England
Temperature Controller with Furnace	FU400	Schnider Electric
Muffle Furnace	M110	Petrotest Germany
FT-IR Spectroscopy	M530	Vuk Sci.
FT-IR Spectroscopy	Carry630	Agilent Technology, USA
XRF	SN9952120	ThermoFisher
GC-MS	7890B	Agilent Technology, USA

The glass wares were washed before and after each stage of experimental works to ensure maximum purity.

2.2 Sample Collection and Treatment

The Melon Seed Husk was obtained from a Local Melon Seed Processing Centre in Nguru Local Government Area of Yobe State. The collected sample was dried under the sun in a dry place, ground, and sieved then stored in a dry place.

2.3 Methods

2.3.1 Reagent Preparations

This section gives detail procedure for the preparation of reagents used.

a. Sulphuric Acid (H_2SO_4) Solution (10%, 8%, 7%, and 5%)

The H_2SO_4 solution (10%) was first prepared by dissolving approximately 26.00 cm^3 of concentrated sulphuric acid in a beaker containing distilled water and the solution was transferred into 250 cm^3 volumetric flask then filled up to the mark with distilled water. the solution was allowed to cool down at room temperature. The H_2SO_4 solution of 8%, 7%, and 5% were prepared by dissolving approximately 21 cm^3 , 18 cm^3 , 13 cm^3 of concentrated sulphuric acid respectively in a beaker containing distilled water and each solution was transferred into 250 cm^3 volumetric flask then filled up to the mark with distilled water.

b. Sodium Hydroxide (NaOH) Solution (4M).

The 4M NaOH was prepared by Weighting Sodium hydroxide pellets (16.000g) and dissolved in 50 cm^3 of distilled water in a small beaker. The solution was then transferred into 100 cm^3 volumetric flask then filled to the mark with distilled water.

2.3.2 Catalyst Preparation

Preparation of NiO/SiO₂ (NiS)

Impregnation of Nickel in the Silica support, The NiO/SiO₂ was prepared by dissolving 2.96g of nickel(II)nitrate(Ni(NO₃)₂.6H₂O) in water added with 5.96g of Silica (SiO₂) composite stirred for 24hours at room temperature, after filtration the precipitate obtained was dried at 120 °Covernight followed by Calcination at 500 °C for 5hours (Zhang *et al.*, 2017).

2.3.3 Catalyst Characterization

The prepared NiO/SiO₂ catalyst was characterized using X-ray Fluorescence (XRF) and The Fourier transform infrared (FT-IR)Spectroscopy.

The Fourier transform infrared (FT-IR) spectroscopic analysis of the prepared NiO/SiO₂ was carried out at the Analytical Chemistry Laboratory, Yobe State University, Damaturu, using M530 model Spectroscopy. The transmission rate was set at the range of 4000-600 cm⁻¹ at 4 cm⁻¹ resolution value. The sample was mixed with alkali halide potassium bromide (KBr) and compressed into a thin transparent pellet using hydraulic press and placed in standard sample compartment of the spectrometer and spectral data was obtained.

The XRF analysis of the NiO/SiO₂ was carried out at the Central Science Laboratory, Umaru Musa Yaradua University, Katsina using ARL QUANT'X EDXRF ANALYSER SN9952120 Model. The sample was mixed with alkali halide potassium bromide (KBr) and compressed into a thin transparent pellet using

hydraulic press and placed in standard sample compartment of the XRF machine and the peaks of the elemental compositions were obtained.

2.3.4 Experimental Design

Response Surface (Central Composite Design) statistical experiment design was used to design the furfural production experiment and the optimization design. Three independent variables namely Temperature ($^{\circ}\text{C}$), Time (Mins), and Acid Concentration (%) were selected for the investigation. Table 2.3 shows the lower and upper levels of the factors employed based on literature survey. (Muhammad *et al.*, 2016; Sokoto *et al.*, 2018).

Table 2.3: Process Variables and their Levels used in the Central Composite Design

Independent Variables	Symbols	Level of Variable	
		Low(-)	High(+)
Temperature ($^{\circ}\text{C}$)	A	150	220
Time (Mins)	B	25	55
Acid Concentration (%)	C	5	10

A total of 20 runs were obtained (Table 3.1). The experiment was design using MINITAB 17 statistical software and the data collected from the experiments was analyzed using same software at $\alpha = 0.05$ (95% confidence level).

2.3.5 Description of the Experimental Runs for Furfural Production

The method described by Sokoto *et al.*, (2018) was adopted for the synthesis of furfural. Each trial involved dried samples (5.0g) of melon seed husk and sodium chloride (NaCl) (5.0g) were mixed in a clean beaker. The mixture was placed into a borosilicate glass tube reactor (250cm³) and dilute sulphuric acid (H₂SO₄) (50cm³ of 10%, 8%, 7% or 5%) as in the design matrix was added into the glass tube. The reactor was placed upright inside furnace and connected to water condenser. The Distillation process was carried out according to the chosen variables of sulphuric acid concentration (%), temperature (°C) and time (mins) as in the design matrix respectively.

The organic portion of the distillate was extracted with dichloromethane using separatory funnel and sodium sulphate (0.2g) was added to remove any trace water in the distillate. The solvent used was removed using rotary evaporator at 40°C. And the resultant solution was analyzed by FT-IR spectroscopy (Sokoto *et al.*, 2018).

To obtain furfural yield (equation (2.1)), the weight of furfural obtained from each run was normalized to the weight of the sample of melon seed husk. (Muhammad *et al.*, 2016; Sokoto *et al.*, 2018).

$$\% \text{Furfural Yield} = \frac{\text{Weight of Furfural formed (g)}}{\text{Dry weight of substrate utilized (g)}} \times 100 \dots \dots \dots (2.1)$$



Plate 2.1: Set up for Furfural Production

Source: Author's Field work 2019

2.3.6 Data Analysis

The furfural yields obtained from the experiments conducted were analyzed on MINITAB 17 Statistical Software to estimate the main and interaction effects on the reaction variables (temperature, time and acid concentration) on the furfural yield. The percentage furfural yield was fitted with a full quadratic polynomial model using regression analysis (equation (2.2)). The fitness of the model was evaluated by the coefficient of determination (R^2) and the effects of terms were evaluated using analysis of variance (ANOVA) at 95% confidence level.

$$Y = b_0 + b_1X_1 + b_2X_2^2 + b_3X_1X_2 \quad (2.2)$$

Where, b_0, b_1, b_2, b_3 are intercept, linear, quadratic, and interaction coefficients respectively.

Contour plots were developed using the fitted quadratic polynomial equation, holding one of the independent variables at a constant value and changing the other variables. Optimizer on the MINITAB 17 was used to optimize the factors and the optimal level obtained was experimentally validated (Muhammad *et al.*, 2016).

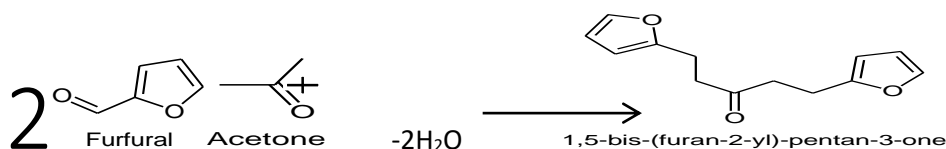
2.3.7 Optimization and Validation of the Furfural Yield

Optimization of the furfural yield was carried out using response optimizer in MINITAB 17 statistical software. Three independent variables namely Temperature, Time and Acid Concentration that affect the furfural yield were optimized in this study to determine the experimental condition that is best for maximization of furfural yield. Further experimental study was carried out for Validation on the reliability of the conditions predicted by the response surface optimizer.

2.3.8 Aldol Condensation of Furfural with Acetone

The aldol condensation of furfural with acetone was performed using a flat bottom flask of 250 cm³ capacity equipped with a magnetic stirrer. Then 10cm³ of the distillate furfural was mixed with 5cm³ of acetone in the ratio of 2:1, and was subsequently transferred into the reactor, where 50% water/Ethanol (v/v) was added to the mixture. The reactor was heated at 85 °C and 20cm³ of 4M NaOH solution was added to the mixture with vigorous stirring (500rpm/min) for 30 minutes.

(Garba *et al.*, 2019). The resulting precipitate was filtered and washed three times with ethanol to remove excess NaOH. Any crystalline products that had formed were dissolved in ethylacetate. The products were analysed using a FT-IR (Garba *et al.*, 2019).



Scheme 2.1: Condensation of Furfural with Acetone

2.3.9 FT-IR Analysis of Furfural Produced and Furfural Acetone Adduct

The FT-IR analysis of produced furfural and aldol adduct was carried out at the Central Science Laboratory UsmanuDanfodiyo University, Sokoto using Carry630 Model Spectroscopy. The transmission rate was set at the range of $4000\text{--}650\text{ cm}^{-1}$ at a resolution of 4 cm^{-1} . A drop of the sample was placed on a thin film positioned in the standard sample compartment of the FT-IR and the spectral data was obtained.

2.3.10 Hydrodeoxygenation of Furfural-Acetone Adduct (FAA) to Hydrocarbon Fuels

Hydrodeoxygenation of the Furfural-Acetone Adduct (FAA) Condensation product was carried out in liquid phase using Stainless steel tubular reactor at 150°C over NiO/SiO_2 catalyst. 5g of the Aldol adduct (FAA) and 0.2g NiO/SiO_2 catalyst and 60 cm^3 of water was transferred into the reactor and the reactor was purged with nitrogen gas. The reactor was pressurized with hydrogen gas at up to 2 bars and heated to 150°C for 8 hours. The liquid product obtained at the end of the

reaction was then filtered and extracted using dichloromethane and analyzed by gas chromatography and mass spectrometry (GC-MS) (Ulfaet *al.*,2019).



Plate 2.2: Set up for Hydrodeoxygenation of Furfural-Acetone adduct to Hydrocarbon fuels

Source: Author's field work 2019

2.3.11 GC-MS Analysis of Hydrodeoxygenated Product

The GC-MS analysis of the hydrodeoxygenated product was carried out at Analytical Chemistry Laboratory Yobe State University, Damaturu on Agilent Technologies GC 7890B, MSD 5977A. The injection volume was 1 μ l and the inlet temperature was maintained at 230°C. The oven temperature was programmed initially at 80°C for 5 min and then programmed to 300°C at the rate of 6 °C and

holding the temperature for 15 min and the total run time was 45 min. The MS transfer line was maintained at 250°C, the source temperature was maintained at 230°C and the MS Quad at 150°C. The ionization mode was set at 70eV. Total Ion Count (TIC) was used to evaluate for compound identification and quantitation. The spectrum of the separated compound was compared with the database of the spectrum of known compound saved in the NIST02 Reference Spectral Library.

CHAPTER THREE

RESULTS AND DISCUSSION

3.1 Effect of the Process Variables on the Furfural Yield

The experiments were performed on furfural production from melon seed husk. Table 2.1 above shows the experimental conditions applied for each treatment condition. 20 runs of experiment and their results were obtained (Table 3.1). At experimental conditions the value of furfural yields varies from 18.72% to 72.86%.

Table 3.1: Central Composite Design for the Furfural Production

Run	Temp.(°C)	Time (Min)	Acid Conc. (%)	FurfuralYield (%)
1	150	25	5	18.72
2	220	25	5	29.64
3	150	55	5	58.40
4	220	55	5	47.12
5	150	25	10	38.00
6	220	25	10	66.13
7	150	55	10	37.61
8	220	55	10	72.86
9	183	40	8	43.72
10	187	40	8	50.40
11	185	39	8	40.06
12	185	41	8	38.02
13	185	40	7	54.42
14	185	40	8	56.30
15	185	40	8	54.70
16	185	40	8	59.66
17	185	40	8	53.08
18	185	40	8	56.66
19	185	40	8	55.46
20	185	40	8	50.92

The ANOVA analysis results (Table 3.2) of the model F-value for furfural yield indicates that the model is significant. The significant of the models are confirmed by relatively higher Fischer's 'F-statistics' value and lower value of probability('P' value) (Chaudhary and Balomajumder, 2014). The results of analysis of variance (ANOVA) in fitting the results (table 3.2) into equation (2.2) reveal that with exception of square terms and interaction of Temperature and Time all other linear and interaction terms of the process variables are all statistically significant ($p < 0.05$, at $\alpha = 0.05$), although with the "lack of fit" (F -value = 7.00) and (p -value = 0.026) implies that the lack of fit of the data is significant ($p < 0.05$). The high coefficient variation ($R^2 = 87.28\%$) show that the model adequately accounts for the empirical relationship between the furfural yield and the process variables.

Table 3.2: Results of Analysis of Variance (ANOVA) for Furfural Yield (%)

Source	DF	Adj SS	Adj MS	F- Value	P-Value
Model	9	2713.92	301.547	8.31	0.001
Linear	3	1465.51	488.502	13.46	0.001
Temp.,(°C)	1	501.40	501.403	13.82	0.004
Time (mins)	1	502.10	502.403	13.84	0.004
Acid Conc. (%)	1	462.00	462.004	12.73	0.005
Square	3	389.30	129.768	3.58	0.055
Temp.,(°C)* Temp.,(°C)	1	0.03	0.029	0.00	0.064
Time (mins)* Time (mins)	1	197.68	197.684	5.45	0.978
Acid Conc.* (%)*Acid Conc. (%)	1	201.84	201.840	5.56	0.042
2-Way Interaction	3	859.11	286.369	7.89	0.040
Temp.,(°C)*Time (mins)	1	28.43	28.426	0.78	0.005
Temp.,(°C)*Acid Conc. (%)	1	507.85	507.848	14.00	0.397
Time (mins)*Acid Conc. (%)	1	322.83	322.834	8.90	0.004
Error	10	362.81	36.281		
Lack-of-Fit	5	317.74	63.548	7.05	0.026
Pure Error	5	45.07	9.013		
Total	19	3076.73			

DF= degree of freedom, Adj SS= adjusted sum of squares, Adj MS= adjusted mean squares, F-Value = F-statistic value.

Regression analyses of the results (Table 3.3) further shows that with the exception of square term of temperature and interaction term of Temperature and time all other linear and square terms of the process variables are statistically significant ($p < 0.05$). On the other hand, all the interaction terms are also statistically significant. Thus, on eliminating the insignificant terms from the model the new regression model (equation (3.1)) with seven significant terms is better than previous model (adjusted $R^2 = 79.86\%$ compared to 77.60%) (Appendix I) with 9 terms.

Table 3.3: Results of Regression Analysis showing the Estimated Coefficients of the Model and their Significance

Term	Effect	Coef	SE Coef	T- Value	P-Value	Significance
Constant		51.12	1.74	29.39	0.000	S
Temp.,(°C)	15.83	7.91	2.13	3.72	0.004	S
Time (mins)	15.84	7.92	2.13	3.72	0.005	S
Acid Conc. (%)	15.19	7.60	2.13	3.57	0.978	ns
Temp.,(°C)*Temp.,(°C)	-78	-39	1391	-0.03	0.042	S
Time(mins)*Time(mins)	-6494	-3247	1391	-2.33	0.042	S
Acid Conc. (%) *Acid Conc. (%)	6562	3281	1391	2.36	0.040	S
Temp.,(°C)*Time (mins)	-3.77	-1.88	2.13	-0.89	0.397	ns
Temp.,(°C)*Acid Conc. (%)	15.94	7.97	2.13	3.74	0.004	S
Time(mins)*Acid Conc. (%)	-12.70	-6.35	2.13	-2.98	0.014	S

S=statistically significant, and ns= statistically not significant, Coeff= regression equation coefficient, SE Coeff= Standard error for coefficients, T-value = t-statistics value.

The four-in-one residual plots (Appendix II) show that the basic requirements of the regression analysis have been met: the residuals are randomly and normally distributed. Because of the apparent skewness of the residuals from the histogram, the normality distribution was confirmed with test for normality (Appendix III) ($p = 0.392$, ($P > 0.05$) Anderson-Darling statistic = 0.369):

Regression Equation

$$\begin{aligned} \text{FurfuralYield}(\%) = & 6108 - 0.1938\text{Temp.}, (^\circ\text{C}) + 1163\text{Time}(\text{mins}) - \\ & 7823\text{Acid Conc.}(\%) - 14.52\text{Time}(\text{mins}) * \text{Time}(\text{mins}) + 522\text{Acid Conc.}(\%) * \\ & \text{Acid Conc.}(\%) + 0.03863\text{Temp.}, (^\circ\text{C}) * \text{Acid Conc.}(\%) - 0.1694\text{Time}(\text{mins}) * \\ & \text{Acid Conc.}(\%) \end{aligned} \quad (3.1)$$

Fig 3.1-3.3 are contour plot describing the relationship between any two of the process variables as they affect the furfural yield while holding the other variable constant.

The furfural yield increased with increasing Acid concentration and reaction Time. At a lower Acid concentration and reaction time (<6%, <30 minutes), the furfural yield was <30%. Highest yields (>70%) are only obtained at Acid concentration >9% and reaction Time 55 minutes. (Fig 3.1)

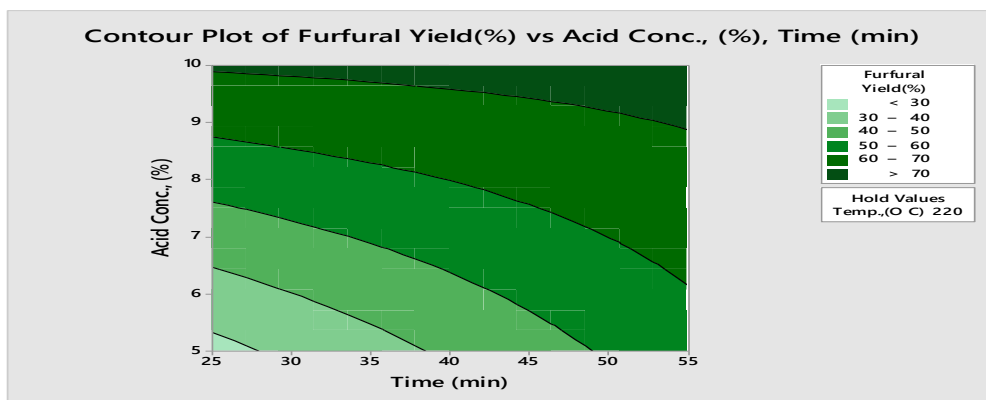


Figure 3.1: Contour Plot Showing the Combined Effect of Acid Concentration and Reaction Time on Furfural Yield with the Reaction Temperature Held Constant.

Acid Concentration and Temperature also interact positively to influence the furfural yield (Fig 3.2). When Acid Concentration is >9% and the Temperature is < 160 °C, the furfural yields is <45%. Maximum yields of the furfural (>70%) are obtained when the distillation process conducted at Acid Concentration (>9%) and Temperature (>210 °C) (Fig. 3.2)

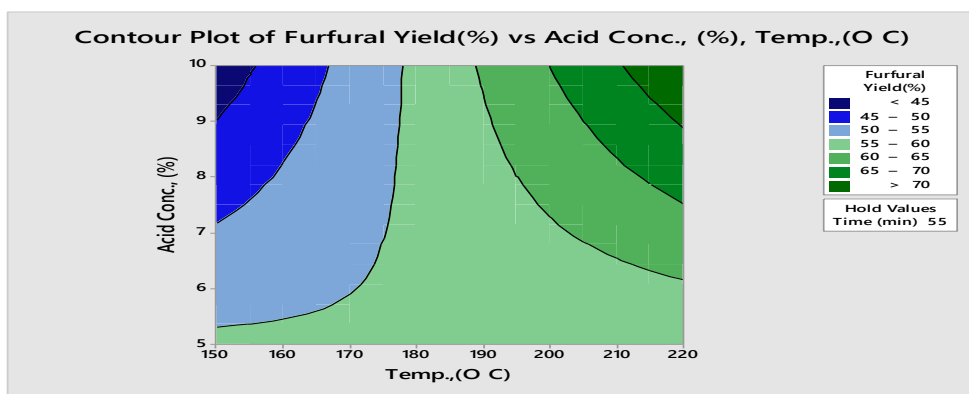


Figure 3.2: Contour Plot Showing the Combined Effect of Acid Concentration and Reaction Temperature on Furfural Yield with the Reaction Time Held Constant

Fig. 3.3 shows the combined effect of the reaction time and temperature on the furfural yield. When the reaction time is <35 minutes and Temperature <160 °C the furfural yield is <40%. The yield increases with an increase in both variables such that, with the reaction performed with Acid Concentration 10%, yields of >70% can only be obtained when the reaction Time is 55 minutes and Temperature is >210 °C (Fig 3.3).

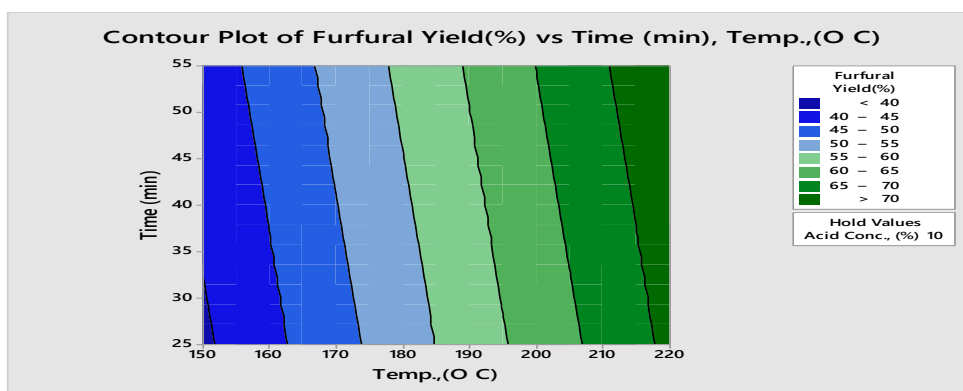


Figure 3.3: Contour Plots Showing the Combined Effect of Reaction Time and Reaction Temperature on Furfural Yield with the Acid Concentration Held Constant

3.2 Response Optimization and Validation

Table 3.3 shows the predicted results for an optimal solution obtained from the optimization. The solution predicted a maximum furfural yield of 74.14% and desirability of 1 with optimal process conditions of temperature, time and Acid concentration of 220° C, 55 minutes and 10% respectively.

Furfural yield of 75.03% was obtained from validation experiment carried out at the levels of the process variables predicted in solution 1. It was observed that the

optimizer predicted and experimental validated results were 74.14 and 75.03% respectively which indicates a relative deviation of 0.89% between experimental validated result and model predicted result. Since the result of the validation result showed agreement with predicted value, the model is reliable (Muhammad *et al.*, 2016). Thus, it can be suggested that the optimization model is reliable and may therefore be more attractive for larger scale furfural production from melon seed husk via acid catalysed hydrolysis/dehydration using Distillation process. Sokoto *et al.*, (2018) reported a maximum yield of 71.55% from millet husk at 184°C for 39 minutes reaction time, 9% acid concentration. Their result is slightly lower yield compare to current work but, it was achieved at lower temperature, time and acid concentration.

Table 3.4: Predicted Result of Optimization and Validation of Melon Seed Husk Furfural Yield

	Temp., (° C)	Time (mins)	Acid (%)	Conc., Furfural Yield (%)	Desirability
Solution					
1	220	55	10	74.1401	1

3.3 Furfural Identification

The produced furfural identity was evaluated using Carry630 Fourier Transform Infra-red (FT-IR). The FT-IR spectrum (Appendix V) shows a very strong absorption at 1670 cm⁻¹. This absorption shows a very significant functional group which corresponds to absorption of conjugated carbonyl (C=O). The C=O

absorption wave number slightly lower than usual (i.e 1740-1720cm⁻¹) absorption of aldehyde due to internal hydrogen bonding which occurs in conjugated unsaturated aldehydes, and conjugation lower the vibrational frequency of carbonyl compounds. The absence of peak at 1725cm⁻¹ indicates strongly the presence of aldehydes not ketone group (Ong and Sashikala, 2007). The presence of the aldehyde group was proven with the existence of two weak absorption observed at 2850 cm⁻¹ and 2800 cm⁻¹ which indicates moderate intense stretching of aldehydic C-H which is attributable to Fermi resonance between the fundamental aldehydic C-H stretching and the first overtone of the aldehydic C-H bending vibration it appears at 1,370cm⁻¹ in the spectrum, these bands are frequently observed for aldehyde group.. In addition, Strong peaks indicated from 1570 cm⁻¹ to 1470 cm⁻¹ are inactive of stretching of C=C from aromatic ring. Aromatic =C-H bending out of plane peaks was observed from 900 to 750. Two strong peaks at 1,160cm⁻¹ and 1,200cm⁻¹ indicated C-O stretching vibration. This IR spectrum was compared with the furfural IR spectrum published by Garbaet *al.*, (2019), Amehet *al.*, (2016), and Ong and Sashikala (2007) and it suits that spectrum.

3.4 Furfural Acetone Adduct Identification

The condensation reaction of furfural with acetone was carried out in a flat-bottomed flask of 250cm³ capacity equipped with magnetic stirrer using NaOH as a catalyst. From the FT-IR analysis of the Furfural-Acetone-Adduct (Appendix VI) obtained, shows the frequency of the main absorption bands illustrates the C-H vibrational frequency which appears at 3140 and 3120 cm⁻¹, correspond to the sp² vibration in the furan ring. The stretching absorbance C=O observed at 1600cm⁻¹

¹inferred the carbonyl group, and a sharp stretching absorbance band at 1010cm⁻¹ probably indicates C-O stretching for cyclic C-O-C linkages of furfural. The peaks at 1450cm⁻¹ and at 1550cm⁻¹ may be as a result of C=C stretching vibration in the furan unit. Similarly, the lower broad absorption at 3400cm⁻¹ could be due to the presence of O-H vibration, which could be attributed to the absorption of the solvent (ethylacetate) that remained in the product. , similar with finding of Garba, et al (2019) and Gandini (2010).

3.5 NiO/SiO₂Catalyst Characterization

The FT-IR spectra for NiO/SiO₂ registered in the range of 600-4000 cm⁻¹ as presented in Appendix VII. Absorption peaks with the FT-IR spectrum of NiO/SiO₂ show the vibrational peaks representing the characteristic metal-oxygen stretching frequencies associated with the vibrations of Ni-O-Si-O and Ni-O-Si bonds. The spectra show a broad band at 3411 cm⁻¹ that is related to the silanolsSiOH stretch vibration (O-H) present on the silica surface (Querem *et al.*, 2018). The bands centred at 1,121.46 and 827.73 cm⁻¹ correspond to the asymmetrical and symmetrical stretch vibration mode associated to the Si-O-Si which is found at 1050cm⁻¹ for pure silica.and stretch Ni-O-Si respectively (Bonakin*et al.*, 2015), finally The absorption peak at 618.45 cm⁻¹ can be associated to the Ni-O. The characteristic absorption of NiO/SiO₂ observed corresponds to the absorption of NiO/SiO₂ reported by Zhang *et al.*, (2013) and Tarafdare*et al.*, (2005).

The percentage of metal analysed by XRF (Appendix VIII) present a relative peak of 73.939% SiO₂support and 24.641% NiO. The result also reveal the presence of

some other element which were also detected at low percent as presented in the table below:

Table 3.5:XRF Results of NiO/SiO₂

Element	Peak(cps/mA)	Relative Peak (%)
SiO ₂	125654	73.939
NiO	41875	24.641
Fe ₂ O ₃	24	0.014
Al ₂ O ₃	890	0.524
MgO	109	0.064
Na ₂ O	2	0.001
SO ₃	363	0.214
P ₂ O ₅	942	0.554
CaO	30	0.018
K ₂ O	2	0.001
TiO ₂	9	0.005
Cr ₂ O ₃	13	0.008
BaO	2	0.001
SrO	2	0.001
Sb ₂ O ₃	6	0.004
Cs ₂ O	5	0.003
ZrO ₂	14	0.008

3.6 GC-MS of Hydrodeoxygenated Product of Furfural Acetone Adduct

The mixture of Furfural Acetone Adduct (FAA) was subjected for direct Hydrodeoxygenation(HDO) using Ni/SiO₂ as a catalyst. The reaction was carried out in a stainless steel tubular reactor using water as solvent. After heated at 150°C for 8hrs, the product was analysed using GC-MS (GC 7890B, MSD5977A, Agilent Technology). Result in Table 3.5 show the distribution of the alkanes obtained from hydrodeoxygenation of aldol adducts. The Hydrodeoxygenation products using Ni/SiO₂ catalyst were detected as the mixture of alkane derivatives and oxygenated product. The products were mainly liquid hydrocarbons with a carbon range C₉-C₁₂. Similar work was reported by Han *et al.* (2015) on hydrodeoxygenation of pyrolysis oil for hydrocarbon production using nanospring based catalysts. Hydrocarbons yields of the Alkanes and Cycloalkenes products obtained from hydrodeoxygenated product over NiO/SiO₂ was 86.61% and 1.46% respectively. Analysis of GC-MS of the product (Appendix VII) showed the products obtained are Nonane, Decane, Dodecane and 2-propenylidenecyclobutene. There were some other organic oxygenates identified by the GS-MS data including 2-butoxy ethanol and 11-(2-cyclopenten-1-yl) undecanoic acid which are most likely by-products. The hydrogenation, ring opening, and deoxygenation reaction was occurred giving the varied products. Wang *et al.* (2015) obtained an experimental yield of more 90% liquid alkanes (aviation fuels range C₈-C₁₅) using Ni/ZrO₂-SiO₂ from raw conorb. Garba *et al.*, (2019) reported 77.50% of liquid hydrocarbons with a carbon range C₁₀-C₂₂ from hydrodeoxygenation of furfural-acetone adducts over NiO/Al₂O₃ obtained from hemicelluloses extract of millet husks.

Table3.6:Composition of HydrodeoxygenatedProduct

Name of Hydrocarbon	Molecular Formula	Molecular Weight(g)
Nonane	C ₉ H ₂₀	128
Decane	C ₁₀ H ₂₂	142
Dodecane	C ₁₂ H ₂₆	170
2-propenylidenecyclobutene	C ₇ H ₈	92

CHAPTER FOUR

CONCLUSION AND RECOMMENDATIONS

4.1 CONCLUSION

Liquid hydrocarbons were produced from Furfural obtained from Hemicellulose of melon seed husk by catalytic hydrodeoxygenation. The pathway involved the simultaneous steps of melon seed husks hydrolysis/dehydration to furfural, Aldol condensation of furfural and acetone to give Furfural-acetone adduct (FAA) and hydrodeoxygenation of the Furfural Acetone Adduct (FAA) to the final hydrocarbons (C_9 - C_{12} alkanes and cycloalkene). The optimum furfural yield of 75.03% was achieved via degradation of hemicellulose fraction of the melon seed husk using H_2SO_4 as catalyst. The NiO/SiO_2 catalyst was produced via impregnation method. The FT-IR of NiO/SiO_2 revealed the presence of functional group Si-O-Si and peak at 618.45 cm^{-1} associated to the Ni-O. 73.939% Silica (SiO_2) and 24.641% NiO was obtained by the XRF analysis of NiO/SiO_2 Catalyst. More than 86% of liquid alkanes and 1.46% cycloalkenes yields was obtained by hydrodeoxygenation of Furfural Acetone adduct (FAA) over NiO/SiO_2 . In the liquid alkanes the main carbon chain was in the ranges of C_9 - C_{12} , both which are suitable for transportation fuels.

4.2 RECOMMENDATIONS

The following are recommendation for future work:

1. Different type of acid (like HCl, and Organic acid) should be adopted for furfural synthesis with the same/different acid concentration to ascertain the optimum yield that could be obtained.
2. The use of different solvents for the extraction of the furfural and hydrocarbon products is recommended in order to ascertain the influence/effect of solvent on furfural and hydrocarbons yields.
3. Effect of the amount of substrate at different mass to the amount of acid at different volume should be investigated for furfural production.
4. Availablenon-edible and inexpensive biomass should be harnessed to find their potentials in generation of biofuels and other value-added chemicals.
5. The condensation process should be optimize to get the desired target product and activity of heterogeneous catalyst should be investigated.

REFERENCES

- Ameh, A.O., Ojo, A.A. and Gaiya, J. (2016). Preliminary Investigation into the Synthesis of Furfural from Sugar Cane Bagasse. *Trend in Science and Technology*, 1, (2), 582-586.
- Baktash, M.M., Ahsan, L. and Ni, Y. (2015). Production of Furfural from an Industrial Pre-Hydrolysis Liquor. *Separation and Purification Technology*, 149, 407-412. <http://dx.doi.org/10.1016/j.seppur.2015.06.003>.
- Barret, C.J., Chhade, J.N., Huber, G.W. and Dumosic, J.A.(2016). Single Reactor Process for Sequential Aldol-condensation and Hydrogenation of Biomass Derived Compounds in Water. *Appl. Catal. B; Environ.*66, 111-118.
- Clark, J.H., Budarin, V., Deswarte, F.E.I., Hardy, J.J.E., Kerton, F.M., Hunt, A.J., Luque, R., Macquarrie, D.J., Milkowski, K., Rodriguez, A., Samuel, O., Tavener, S.J. White, R.J. and Wilson, A.J. (2006). *Greenhouse Chemistry*, 8, 853-860.
- Corma, A., De La Torre, O. and Renz, M., (2012). Production of high quality diesel from cellulose and hemicellulose by the sylvan process. Catalysts and Process Variables. *Energy Environment of Science*.5, 6328-6344.
- Chaudhary, N. and Balomajumder, C. (2014). Optimization Study of Adsorption Parameters for Removal of Phenol on Aluminum Impregnated Fly Ash using Response Surface Methodology. *Journal of Taiwan Institute of Chemical Engineering*. 45, 852e859.
- Chen, H., Qin, L. and Yu, B. (2015). Furfural Production from Steam Explosion Liquor of Rice Straw by Solid Acid Catalysts (HZSM-5). *Biomass and Bioenergy*. 73, 77-83. <http://dx.doi.org/10.1016/j.biombioe.2014.12.013>.
- Corma, A., Iborra, S. and Velty, A.(2007). Chemical Routes for the Transformation of Biomass into Chemicals. *Chemistry Review*. 107, 6 2411-502.
- Corma, A., Maria, J.C. and Sara, I. (2014). Conversion of Biomass Platform Molecules into Fuel Additives and Liquid Hydrocarbon Fuels. *Green Chemistry*. 16, 516-547.
- Faba, L., Díaz, E. and Ordóñez, S.(2012). Aqueous-phase Furfural-acetone Aldol Condensation over Basic Mixed Oxides *Applied Catalysis. B* 113 201-11.
- Faba, L., Díaz, E. and Ordóñez, S. (2014). Hydrodeoxygenation of Acetone - furfural Condensation Adducts Over Alumina-supported Noble Metal Catalyst. *Applied Catalysis B*. 160 436-44.
- Faba L, Díaz, E., Vega, A. and Ordóñez, S.(2016). Hydrodeoxygenation of Furfural-acetone Condensation Adducts to Tridecane over Platinum Catalysts. *Catalysts Today* 269 132-9.

- Gandini, A. (2010). Furans as Offspring of Sugars and Polysaccharides and Progenitors of a Family of Remarkable Polymers: A Review of Recent Progress. *Polymer Chemistry*. 1, 245.
- Garba, N.A., Muduru, I.K., Sokoto, A.M. and Dangoggo, S.M. (2019). Production of Liquid Hydrocarbons From Millet Husk Via Catalytic Hydrodeoxygenation In NiO/Al₂O₃ Catalysts *WIT Transactions on Ecology and the Environment*. 222, WIT Press doi:10.2495/EQ180121
- Gao, H., Liu, H., Pang, B., Yu, G., Du, J., Zhang, Y., Wang, H. and Mu, X. (2014). Production of Furfural from Waste Aqueous Hemicellulose Solution of Hardwood over ZSM-5 Zeolite. *Bioresource Technology*. 172, 453-456. <http://dx.doi.org/10.1016/j.biortech.2014.09.026>.
- Gebre, H., Fish, K., Kindeya, T. and Gebremichael, T. (2015). Synthesis of Furfural from Bagasse. *International Letters of Chemistry, Physics and Astronomy*, 57, 72-84. doi:10.18052/www.scipress.com/ILCPA.57.72.
- Han, Y., McIlroy, D.N. and McDonald, A.G. (2015). Hydrodeoxygenation of Pyrolysis Oil for Hydrocarbon Production using Nanospring Based Catalyst. *Journal of Analytical and Applied Pyrolysis*, <http://dx.doi.org/10.1016/j.jaap.2015.12.011>.
- Huber, G.W., Iborra, S. and Corma, A. (2006). Synthesis of Transportation Fuels from Biomass: *Chemistry, Catalysts, and Engineering*. *Chemical Review*, 106: 4044-4098.
- Kamimoto, M., (2008). The Significance of Liquid Fuel Production from Woody Biomass. Biomass energy 2008-3 issue of AIST TODAY.
- Li, H., Ren, J., Zhong, L., Sun, R. and Liang, L. (2015). Production of Furfural from Xylose, Water-Insoluble Hemicelluloses and Water-Soluble Fraction of Corn cob via a Tin-Loaded Montmorillonite Solid Acid Catalyst. *Bioresource Technology*, 176, 242-248. <http://dx.doi.org/10.1016/j.biortech.2014.11.044>.
- Machado, G., Leon, S., Santos, F., Lourega, R., Dullius, J., Mollmann, M.E. and Eichler, P. (2016). Literature Review on Furfural Production from Lignocellulosic Biomass; *Natural Resources*, 2016, 7, 115-129. <http://dx.doi.org/10.4236/nr.2016.73012>.
- Mahfud, A., Ulfa, S.M. and Utomo, E.P. (2016). Hydrogenation/Deoxygenation (H/D) Reaction of Furfural-Acetone Condensation Product using Ni/Al₂O₃-ZrO₂. Catalyst. *Journal of Pure and Applied Chemistry Resources*. 5(2), 108.
- Muhammad, A.B., Obianke, M., Hassan, L.G. and Aliero, A.A. (2016). Optimization of Process Variables in Acid Catalysed In situ Transesterification of Hevea Brasiliensis (Rubber Tree) Seed Oil into Biodiesel, *Biofuels*, DOI: 10.1080/17597269.2016.1242689.

- Muhammad, C., Onwudili, J.A. and Williams, P.T.(2015). Thermal Degradation of Real-World Waste Plastics and Simulated Mixed Plastics in a Two-Stage Pyrolysis-Catalysis Reactor for Fuel production. *Energy and Fuels* 2015, 29,4, 2601-2609. <https://doi.org/10.1021/ef502749h>.
- Nyakuma, B.B. (2015). Thermogravimetric and Kinetic Analysis of Melon (*Citrullus colocynthis* L.) Seed Husk using the Distributed Activation Energy Model. *Environmental and Climate Technologies* 15(1), 77-89.
- Ong, H.K. and Sashikala, M. (2007). Identification of Furfural Synthesized from Pentosan in Rice Husk. *Journal of Tropical Agriculture and Food Science*. 35(2), 305–312.
- Onwudili, J.A., Muhammad, C. and Williams, P.T. (2018). Influence of Catalyst Bed Temperature and Properties of Zeolite Catalysts on Pyrolysis-Catalysis of a Simulated Mixed Plastics Sample for the Production of Upgraded Fuels and Chemicals. *Journal of the Energy Institute*. <https://doi.org/10.1016/j.joei.2018.10.001>.
- Pushkarev, V.V., Mussel White, N., An, K., Alayoglu, S. and Somorjai, G.A. (2012). High Structure Sensitivity of Vapor Phase Furfural Decarbonylation /hydrogenation Reaction Network as a Function of Size and Shape of Pt Nanoparticles. *Nano Letters*. 12, 5196-5201.
- Perlack, R.D., Wright, L.L., Turhollow, A.F., Graham, R.L., Stokes, B.J. and Erbach, D.C. (2005). Biomass as Feedstock for a Bioenergy and Bioproducts Industry: *The Technical Feasibility of a Billion-Ton Annual Supply; Report No. DOE/GO-102995-2135*; Oak Ridge National Laboratory: Oak Ridge, TN,; <http://info.ornl.gov/sites/publications/Files/Pub57812.pdf>.
- Rong, X., Ayyagari, V., Subrahmanyam, H.O., Wei, Q., Peter, V.W., Hemant P. and Huber, G.W.(2010). Production of Jet and Diesel Fuel Range Alkanes from Waste Hemicellulose-Derived Aqueous Solutions. *Journal of Royal Society of Chemist*, 140: 77-84.
- Seo, J., Kwon, J.S., Choo, H., Choi, J.W., Jae, J., Suh, D.J., Kim, S. and Ha, J.M. (2018). Production of Deoxygenated High Carbon Number Hydrocarbons from Furan Condensates: Hydrodeoxygenation of Biomass-based Oxygenates, *Chemical Engineering Journal*, doi: <https://doi.org/10.1016/j.cej.2018.09.146>.
- Sokoto, A.M., Muduru, I.K., Dangoggo, S.M., Anka, N.U. and Hassan L.G., (2018). Optimization of Furfural Production from Millet Husk using Response Surface Methodology, *Energy Sources, Part A: Recovery, Utilization, and Environmental Effects*. 40:1, 120-124, DOI: 10.1080/15567036.2017.1405120
- Sitthisa, S., An, W. and Resasco, D.E.(2011). Selective Conversion of Furfural to Methylfuran over Silica-supported Ni-Fe Bimetallic Catalyst. *Journal of catalysis*, 284, 90-101.

- Tarafdar, A., Panda, A.B. and Pramanik, P. (2005). Synthesis of ZrO₂-SiO₂ Mesocomposite with High ZrO₂ Content via a Novel Sol-gel Method. *Microporous and Mesoporous Materials*, 84 (1-3), 223-228.
- Ulfa, S.M., Mahfud, A., Nabilah, S. and Rahman, M.F. (2017). Influence of Solvent on Liquid Phase Hydrodeoxygenation of Furfural Acetone Condensation Adduct using Ni/Al₂O₃-ZrO₂ catalyst. IOP conf. series: *Material Science and Engineering* 172. 01 2053 doi: 10.1088/1757-899x/172/1/012053.
- Ulfa, S.M., Prihartin, D., Mahfud, A. and Munandar, R. (2019). Hydrodeoxygenation of Furfural-acetone Condensation Adduct Over Alumina-zirconia and Silica Supported Nickel Catalyst. *Material Science and Engineering*. 509, 012132 doi: 10.1088/1757-899X/509/1/012132.
- Ulfa, S.M., Sari, I., Kusumaningsih, C.P. and Rahman, M.F. (2015). Structural Properties of Ni/ γ -Al₂O₃ and Cu/ γ -Al₂O₃ Catalyst and its Application for Hydrogenation of Furfurylidene Acetone. *Procedia Chem.* 16 616-22.
- Wang, W., Ren, J., Li, H., Deng, A. and Sun, R. (2015). Direct Transformation of Xylan-Type Hemicelluloses to Furfural via SnCl₄ Catalysts in Aqueous and Biphasic Systems. *Bioresources Technology*. 183, 188-194. <http://dx.doi.org/10.1016/j.biortech.2015.02.068>.
- Worldwatch Institute. (2017). The Miracle Melon (Egusi) [Online]. Washington DC: WorldWatch Institute. Available: <https://goo.gl/7I1txD> [Accessed 7th May 2019].
- Yantao, W., Deyang, Z., Daily, R.P. and Christoph, L. (2019). Recent Advances in Catalytic Hydrogenation of Furfural; *Catalysts*. 9(10), 796; <http://doi.org/10.3390/Catal9100796>.
- Zhang, X., Zhang, Q., Chen, L., Xu, Y., Wang, T. and Ma, L. (2014). Effect of Calcination Temperature of Ni/SiO₂-ZrO₂ Catalyst on its Hydrodeoxygenation of Guaiacol. *Chinese Journal of Catalyst*. 35(3), 302-9.
- Zhang, X., Zhang, Q., Wang, T., Ma, L., Yu, Y. and Chen, L. (2013). Hydrodeoxygenation of Lignin-derived Phenolic Compounds to Hydrocarbons over Ni/SiO₂-ZrO₂ Catalysts. *Bioresources Technology*. Apr; 134:73-80.
- Zhang, X., Zhang, Q., Wang, T., Ma, L. and Tang, W. (2017). Hydrodeoxygenation of Lignin-derived Phenolic Compounds to Hydrocarbons Fuel over Supported Ni-based Catalysts. *Applied Energy*, <http://dx.doi.org/10.1016/j.apenergy.2017.08.078>.

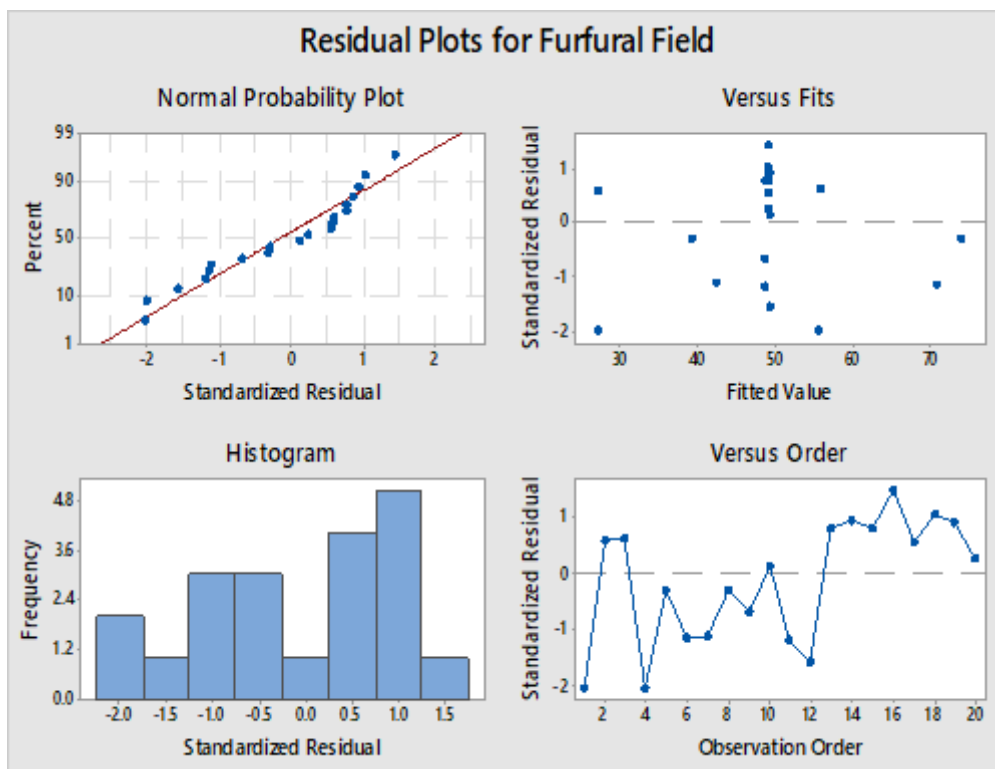
APPENDICES

Appendix I: Model Summary

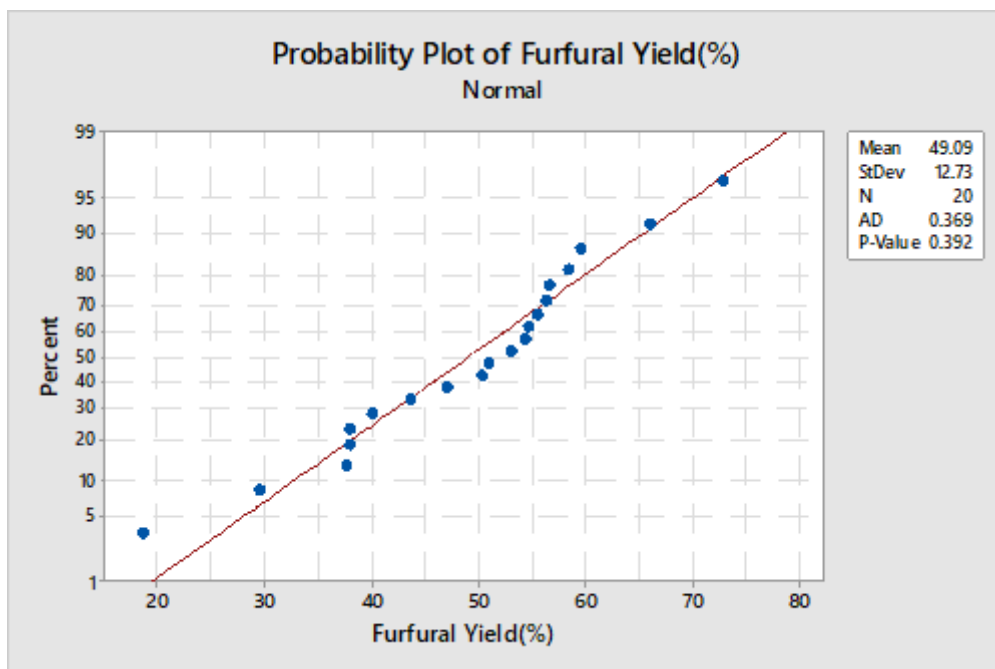
Model Summary

S	R-sq	R-sq(adj)	R-sq(pred)
5.71011	87.28%	79.86%	17.31%

Appendix II: Four-in-One Residual Plots for Furfural Yield(%)



Appendix III: Probability Plot for Normality Test



Appendix IV: Optimization Plot



Appendix V: FT-IR Spectrum of Furfural Produced



Sample ID:Furfural 2 Umar Abba Aji

Method

Name:C:\Users\Public\Documents\Agilent\MicroLa
b\Methods\Aminu 3.a2m

Sample Scans:32

User:Central Lab

Background Scans:64

Date/Time:07/12/2019 12:50:29 PM

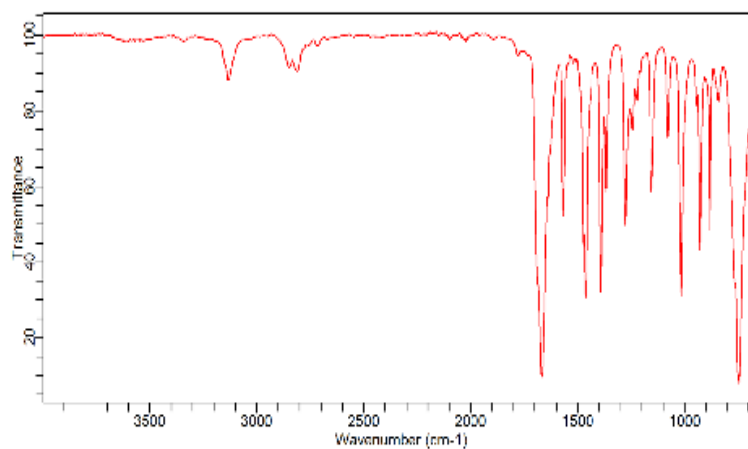
Resolution:4

Range:4000 - 650

System Status:Good

Apodization:Happ-Genzel

File Location:C:\Users\Public\Documents\Agilent\MicroLab\Results\Furfural 2 Umar Abba Aji_0000.a2r



7/12/2019 12:53:37 PM

page 1 of 1

Appendix VI: FT-IR Spectrum of Furfural-Acetone Adduct (FAA)



Sample ID: Adol Aduct 2 Umar Abba Aji

Method

Name: C:\Users\Public\Documents\Agilent\MicroLab\Methods\Aminu 3.a2m

Sample Scans: 32

User: Central Lab

Background Scans: 64

Date/Time: 07/12/2019 12:48:30 PM

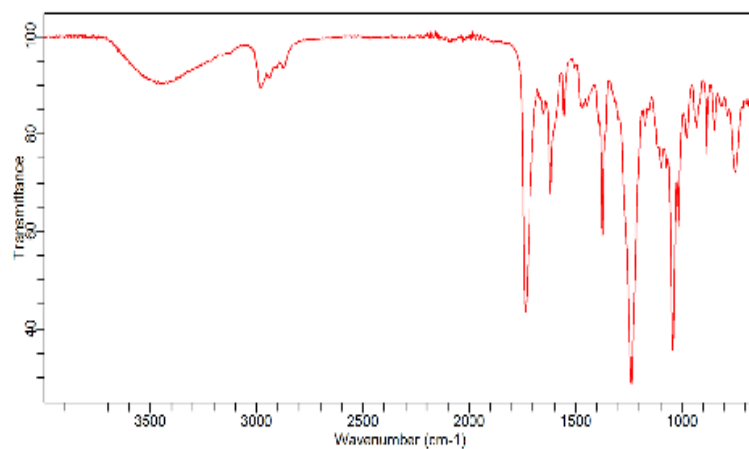
Resolution: 4

Range: 4000 - 650

System Status: Good

Apodization: Happ-Genzel

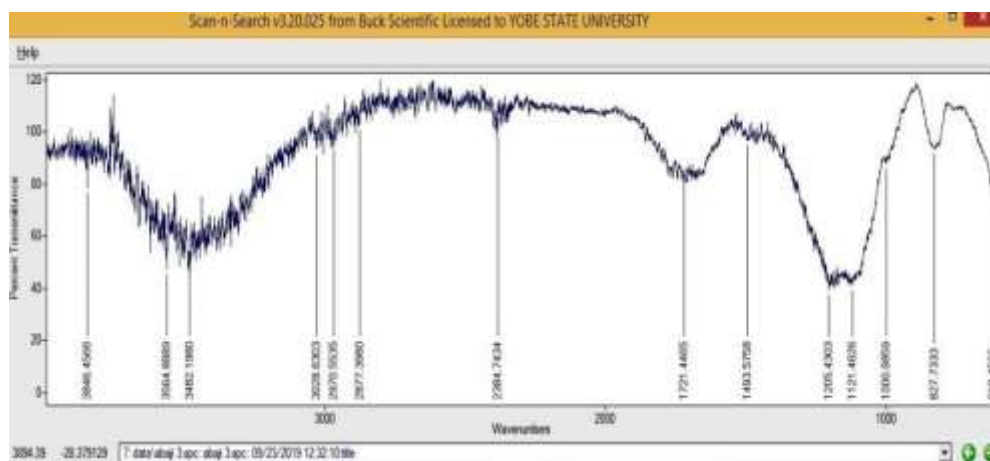
File Location: C:\Users\Public\Documents\Agilent\MicroLab\Results\Adol Aduct 2 Umar Abba Aji_0000.a2r



7/12/2019 12:54:26 PM

page 1 of 1

Appendix VII: FT-IR Spectrum of NiO/SiO₂ Catalyst



Appendix VIII: XRF Result of Ni/SiO₂ Catalyst

Voltage	40 kV	Current	Auto
Livetime	60 seconds	Counts Limit	0
Filter	Cu Thin	Atmosphere	Vacuum
Maximum Energy	40 keV	Count Rate	Medium
Warmup time	0 seconds		

Results				
Element	Concentration	Uncertainty	Peak(cps/mA)	Background(cps/mA)
NiO ₂ and SiO ₂				
Fe ₂ O ₃	0.00428 %	0.00033	24	23
CuO	0 %	0.0	0	870
HgO	0 %	0.0	0	40
NiO	0 %	0.0	41875	-1541
Oy ₂ O ₃	0 %	0.0	0	37
Eu ₂ O ₃	0 %	0.0	0	13
Li ₂ O ₃	0 %	0.0	0	4317
Ta ₂ O ₅	0 %	0.0	0	4328
Tb ₄ O ₇	0 %	0.0	0	35
ZnO	0 %	0.0	0	14
Yb	0 %	0.0	0	36598
Ga ₂ O ₃	0 %	0.0	0	14
HfO ₂	0 %	0.0	0	132
Hu ₂ O ₃	0 %	0.0	0	19
Al ₂ O ₃	0.991 %	0.014	890	1975
MgO	0.1887 %	0.0078	109	275
Na ₂ O	[0.0032] %	0.0052	2	84
SO ₃	0.0514 %	0.0013	363	1146
SiO ₂	88.894 %	0.049	125654	-3367
P ₂ O ₅	0.5038 %	0.0053	942	-375
CaO	0.01009 %	0.00065	30	14
K ₂ O	[0.00099] %	0.00067	2	15
TiO ₂	0.00187 %	0.00036	9	17
MnO	0 %	0.0	0	176
V ₂ O ₅	0 %	0.0	0	32
Cr ₂ O ₃	0.00116 %	0.00031	13	84
La ₂ O ₃	0 %	0.0	0	21
Sc ₂ O ₃	0 %	0.0	0	20
As ₂ O ₃	[0.00030] %	0.00030	0	2
BaO	[0.7] %	1.6	2	197
CdO	0 %	0.0	0	33
PbO	0 %	0.0	0	2
Rb ₂ O	[0.00016] %	0.00019	0	2
SrO	0.00093 %	0.00020	2	2
SeO ₂	[0.00026] %	0.00044	0	3
ThO ₂	0 %	0.0	0	2
U ₃ O ₈	0 %	0.0	0	2
Y ₂ O ₃	0 %	0.0	0	2
Br	0 %	0.0	0	3
MoO ₃	0 %	0.0	0	3
Sb ₂ O ₃	[0.0063] %	0.0049	6	110
Ca ₃ O ₄	0 %	0.0	0	40
Ca ₂ O	[0.0055] %	0.0067	5	218
CeO ₂	0 %	0.0	0	25
ZrO ₂	0 %	0.0	14	5

GENERAL LAB.

UNIVERSITY OF ADUA

25/03/19

Appendix IX: GC-MS Chromatogram of Hydrodeoxygenation Product

YOBE STATE UNIVERSITY DAMATURU



FACULTY OF SCIENCE
DEPARTMENT OF CHEMISTRY
CHEMISTRY ANALYTICAL LABORATORY

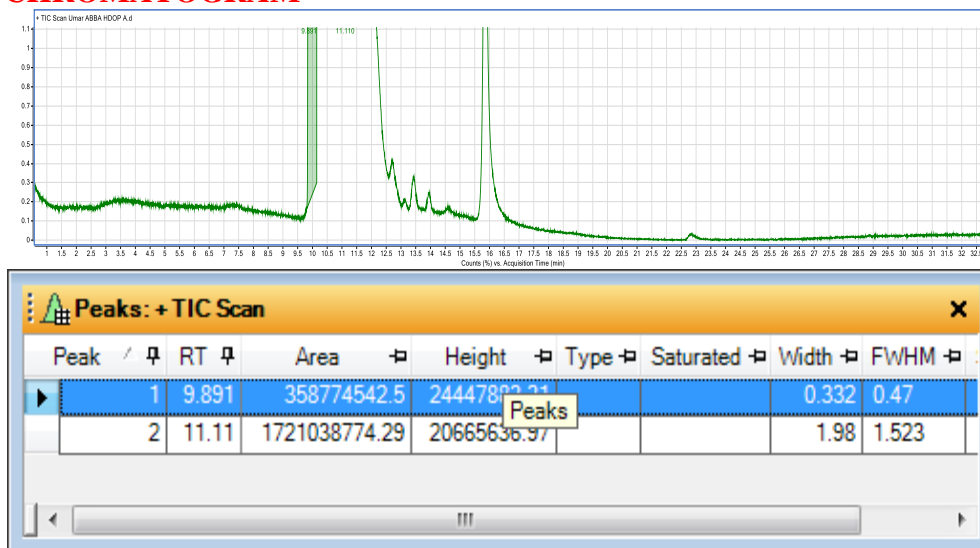
GCMS ANALYSIS RESULTS

(GC 7890B, MSD 5977A, Agilent Tech)

Umar Abba Aji@UDUS

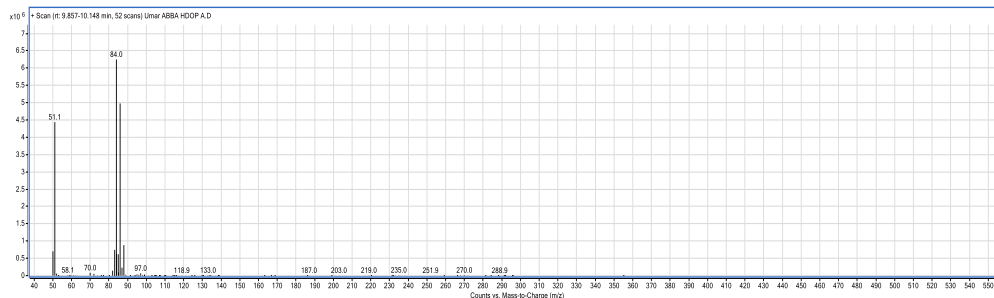
SAMPLE NAME: HDOP

CHROMATOGRAM

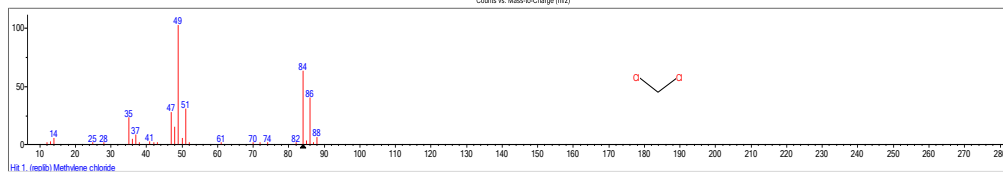
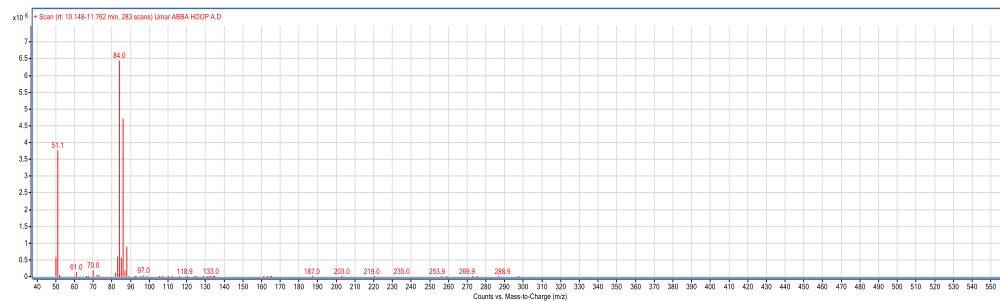


MASS SPECTRA/NIST LIBRARY COMPARISON

PEAK1



PEAK 2



Name: Methylene chloride

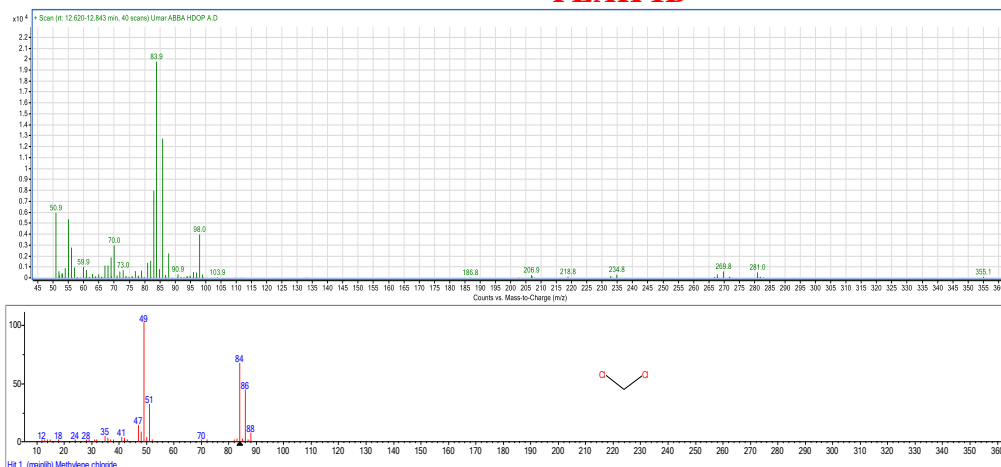
Formula: CH₂Cl₂

MW: 84 Exact Mass: 83.9533553

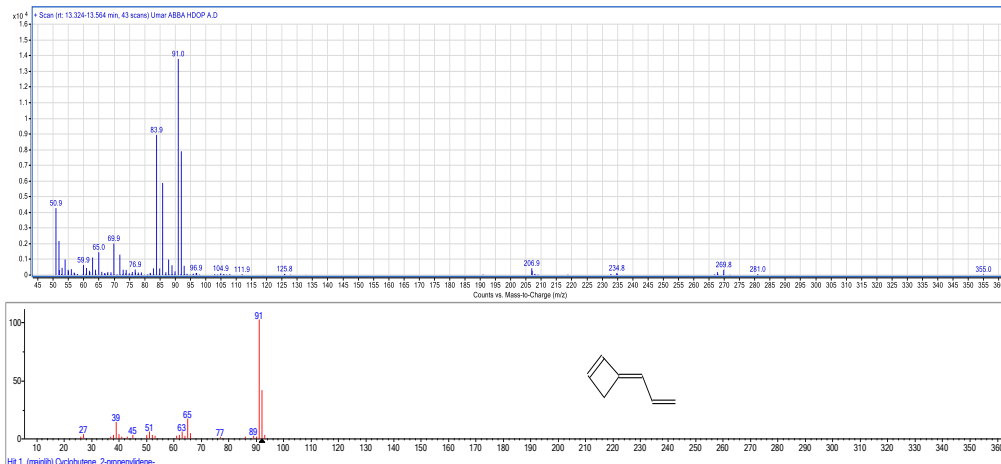
OTHER PEAKS

Peaks: + TIC Scan								
Peak	RT	Area	Height	Type	Saturated	Width	FWHM	
1	12.7	216467.09	26785.31			0.235	0.132	
2	13.42	353150.28	40030.15			0.29	0.141	
3	13.95	174413.01	23728.08			0.229	0.124	
4	14.59	105233.32	10211.03			0.332	0.619	
5	15.85	6227531.49	510027.4			0.761	0.156	
6	22.85	113078.66	7474.63			0.515	0.263	

PEAK 1B



PEAK2B



Name: Cyclobutene, 2-propenylidene-

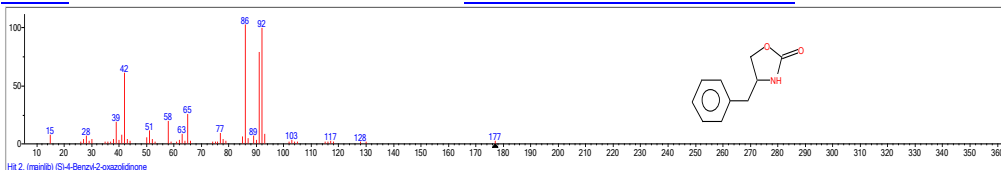
Formula: C₇H₈

MW: 92

Exact

Mass:

92.0626

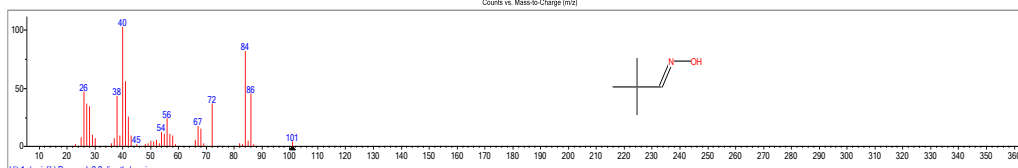
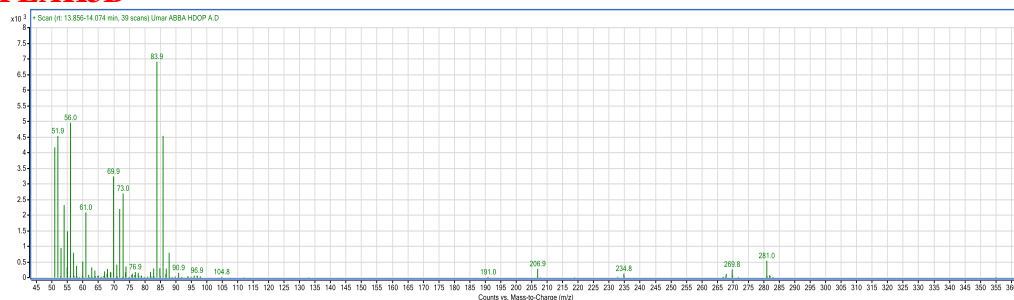


Name: (S)-4-Benzyl-2-oxazolidinone

Formula: C₁₀H₁₁NO₂

MW: 177 Exact Mass: 177.078979

PEAK3B

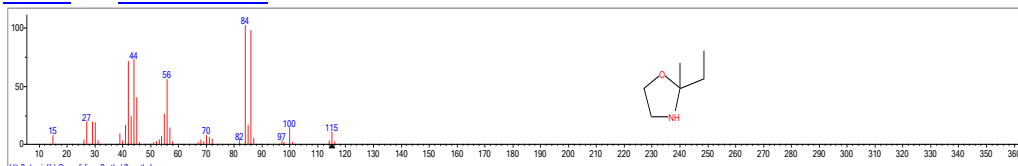


HR 1. (m/z) Propanal, 2,2-dimethyl-, oxime

Name: Propanal, 2,2-dimethyl-, oxime

Formula: C₅H₁₁NO

MW: 101 **Exact Mass:** 101.084064

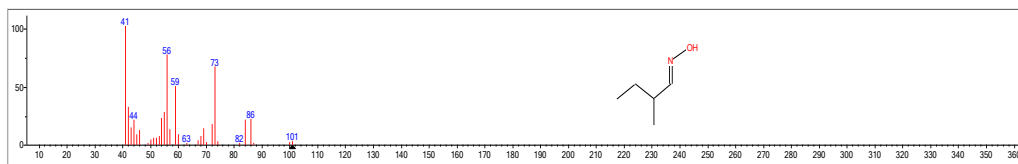


HR 2. (m/z) Oxazolidine, 2-ethyl-2-methyl-

Name: Oxazolidine, 2-ethyl-2-methyl-

Formula: C₆H₁₃NO

MW: 115 **Exact Mass:** 115.0997143



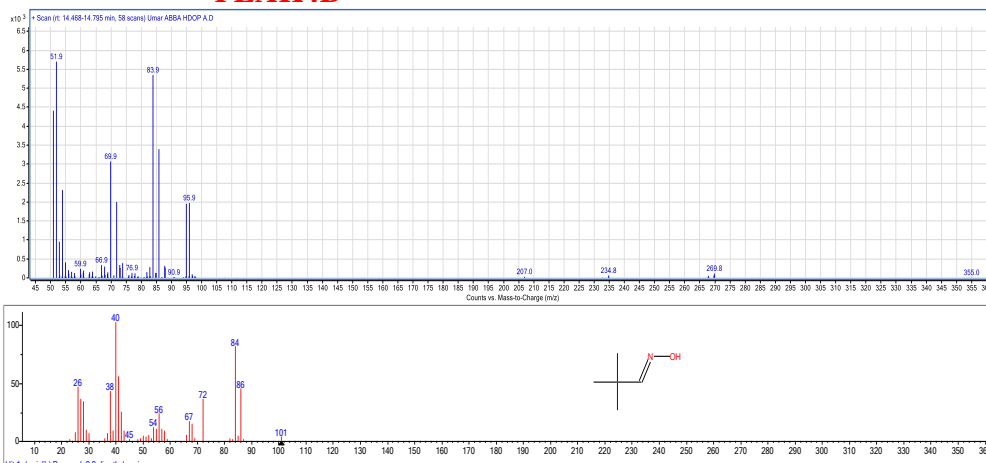
HR 3. (m/z) Butyl aldoxime, 2-methyl-, anti-

Name: Butyl aldoxime, 2-methyl-, anti-

Formula: C₅H₁₁NO

MW: 101 **Exact Mass:** 101.084064

PEAK4B



Hit 1, mainlib) Propanal, 2,2-dimethyl-, oxime

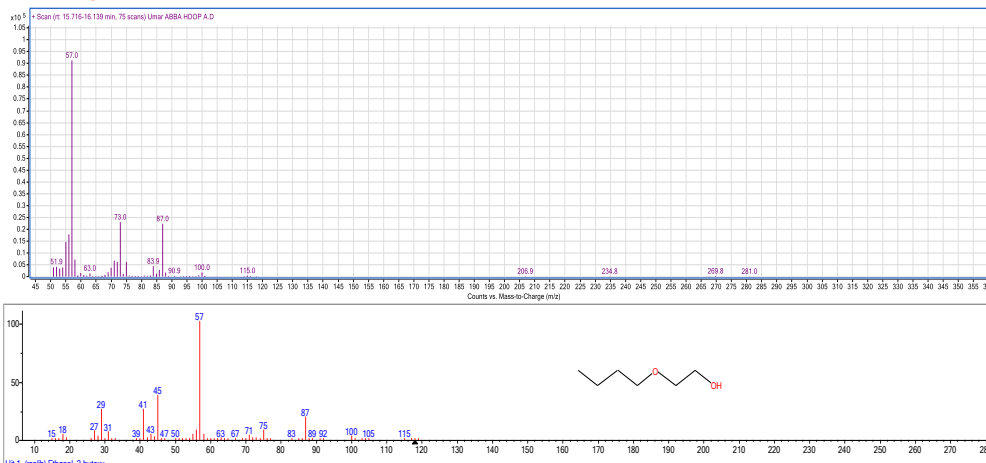
Name: Propanal, 2,2-dimethyl-, oxime

Formula: C₅H₁₁NO

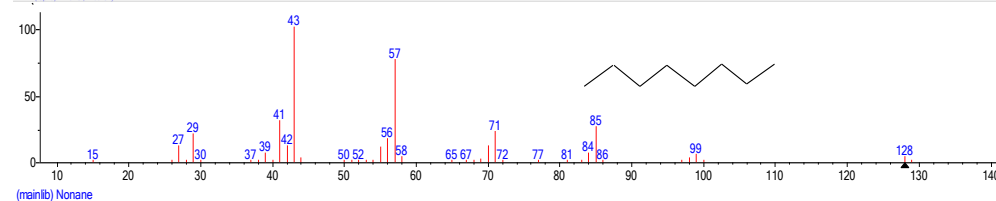
MW: 101 **Exact Mass:** 101.084064 **CAS#:** 637-91-2 **NIST#:** 46275 **ID#:** 1861

DB: mainlib

PEAK5B



Hit 1, mainlib) Ethanol, 2-butanol



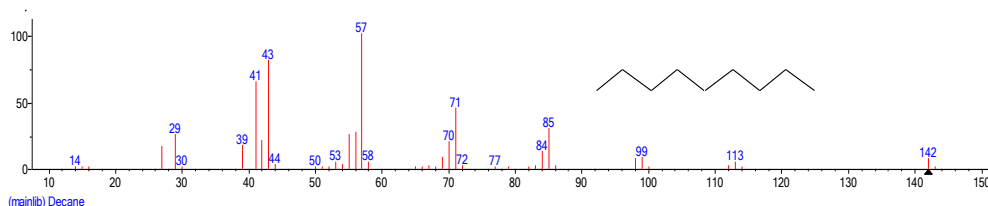
(mainlib) Nonane

Name: Nonane

Formula: C₉H₂₀

MW: 128 **Exact Mass:** 128.156501 **CAS#:** 111-84-2 **NIST#:** 228006 **ID#:** 7287

DB: mainlib



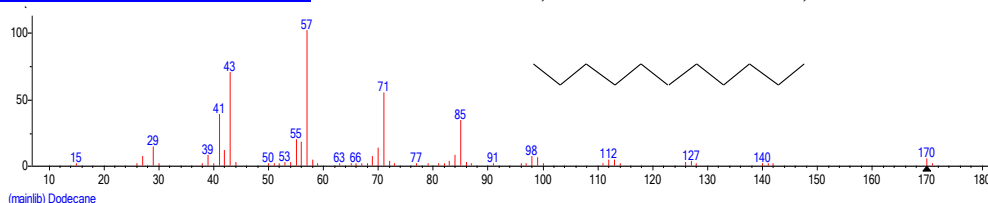
Name: Decane

Formula: $C_{10}H_{22}$

MW: 142 Exact Mass: 142.172151 CAS#: 124-18-5 NIST#: 114147 ID#: 22349

DB: mainlib

Other DBs: Fine, TSCA, RTECS



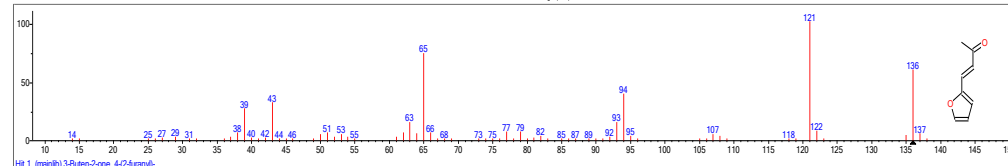
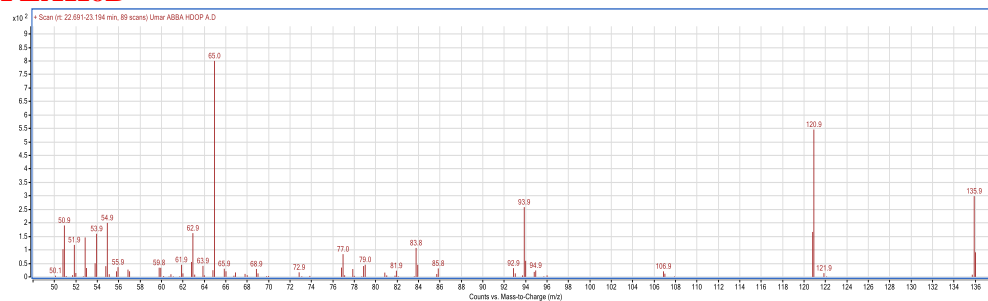
Name: Dodecane

Formula: $C_{12}H_{26}$

MW: 170 Exact Mass: 170.203451 CAS#: 112-40-3 NIST#: 291499 ID#: 22550

DB: mainlib

PEAK6B



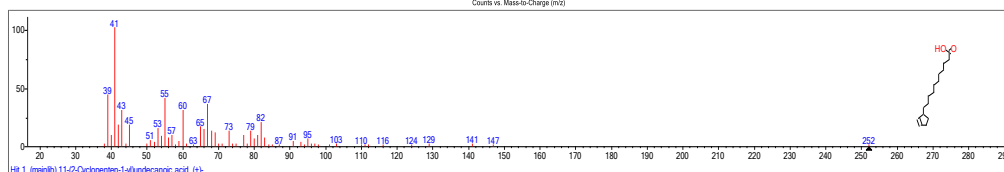
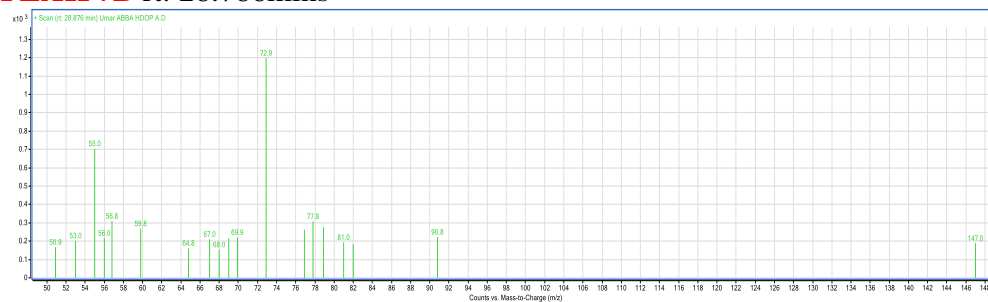
Name: 3-Buten-2-one, 4-(2-furanyl)-

Formula: $C_8H_8O_2$

MW: 136 Exact Mass: 136.052429 CAS#: 623-15-4 NIST#: 341365 ID#: 91533

DB: mainlib

PEAK 7B rt: 28.786mins



Name: 11-(2-Cyclopenten-1-yl)undecanoic acid, (+)-

Formula: C₁₆H₂₈O₂

MW: 252 **Exact Mass:** 252.20893 **CAS#:** 459-67-6 **NIST#:** 12245 **ID#:** 1990

DB:mainlib